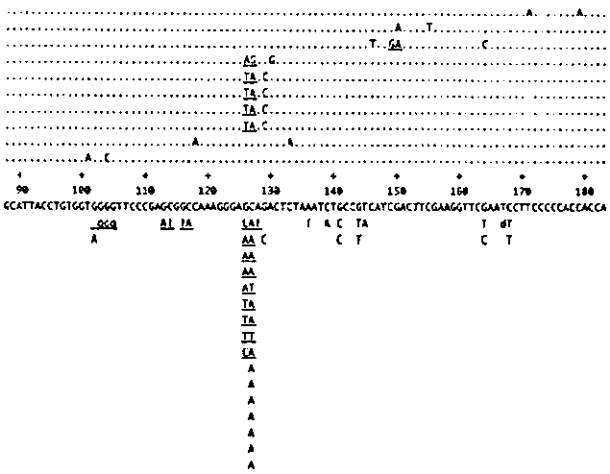

Figure 2. Mutation spectrum of acetaldehyde-treated single-stranded pMY189 replicated in VA13 cells. The location and nature of independent single and tandem (underlined) mutations are indicated below the sequence. The dashed lines above the *supF* sequence represent independent mutants carrying multiple mutations. Several tandem substitutions, present in these multiple mutants, are underlined. The 'd' denotes deletion. The 'ggg' at the region from 102 to 105 bp represents a GGGG to GGG base change. Another multiple mutation found in the other region of *supF* gene was tandem GC(78, 79) to TA and C(127) to A.

Table 3. Types of single-base substitution in the *supF* gene in acetaldehyde-treated shuttle vector

| Double-stranded | | Single-stranded | |
|---|---|---|---|
| Type of mutation | No. of mutations (%) | Type of mutation | No. of mutations (%) |
| G:C to T:A | 9 (37.5) | G to T | 8 (40) |
| | | C to A | 3 (15) |
| G:C to C:G | 13 (54.2) | G to C | 0 (0) |
| | | C to G | 4 (20) |
| G:C to A:T | 2 (8.3) | G to A | 2 (10) |
| | | C to T | 1 (5) |
| A:T to T:A | 0 (0) | A to T | 1 (5) |
| | | T to A | 1 (5) |
| Total | 24 (100) | Total | 20 (100) |

## High sensitivity of nucleotide-excision repair deficient cells to acetaldehyde

We compared the acetaldehyde sensitivity between normal (WI38-VA13) and nucleotide excision repair-deficient [XP2OS(SV)] cell lines (Fig. 4). XP2OS(SV) cells were slightly sensitive to acetaldehyde compared with the normal cells. To eliminate those effects of metabolism and cell toxicity that were not due to DNA damage by acetaldehyde, we examined the survival and mutations of acetaldehyde-treated double-stranded shuttle vectors propagated in both WI38-VA13 and XP2OS(SV) cells (Fig. 5). Survival of the plasmids extracted from XP2OS(SV) was much lower than that of plasmids from WI38-VA13 cells, and the mutation frequency in XP2OS(SV) cells at 0.5 M was five times higher than in WI38-VA13 cells. These results suggest that the DNA damage induced by acetaldehyde can be repaired by the nucleotide excision repair pathway.

Table 4. Types of acetaldehyde-induced tandem base substitution in the *supF* gene in double-stranded shuttle vector plasmids pMY189 propagated in human fibroblast cells WI38-VA13

| Type of mutation | No. of mutations | % |
|---|---|---|
| GG to TT (CC to AA) | 40 | 61 |
| GC to AA (GC to TT) | 7 | 11 |
| GG to AT (CC to AT) | 6 | 9 |
| GG to CT (CC to AG) | 3 | 5 |
| GG to AA (CC to TT) | 2 | 3 |
| GG to TA (CC to TA) | 2 | 3 |
| GC to AT (GC to AT) | 2 | 3 |
| CG to GA (CG to TC) | 2 | 3 |
| CG to AA (CG to TT) | 1 | 2 |
| GA to TT (TC to AA) | 1 | 2 |
| Total | 66 | 100 |

Table 5. Types of acetaldehyde-induced tandem base substitution in the *supF* gene in single-stranded shuttle vector plasmids pMY189 propagated in human fibroblast cells WI38-VA13

| Type of mutation | No. of mutations | % |
|---|---|---|
| GC to TA | 8 | 47 |
| GC to TT | 3 | 18 |
| GC to AT | 2 | 12 |
| GC to AA | 1 | 6 |
| GC to TG | 1 | 6 |
| GC to CT | 1 | 6 |
| CG to TC | 1 | 6 |
| Total | 17 | 100 |

## Binding of XP-A protein to acetaldehyde-treated DNA

The $^{32}$P-labeled DNA was treated with acetaldehyde at a concentration of 0, 0.5 and 1 M for 1 h at 37°C and incubated with various amounts of XP-A protein. If the DNA binds to the XP-A protein, radioactivity remains the on filter. As indicated in Figure 6, binding of the XP-A protein to the acetaldehyde treated DNA is dependent on the amount of XP-A protein and the acetaldehyde concentration. When no XP-A protein was added to the reaction mixture, the radioactivity retained by the filter was 0.6, 2.9 and 14.6% for acetaldehyde concentrations of 0, 0.5 and 1 M, respectively. When 10 and 20 ng XP-A protein were added, this was increased to 2.7, 8.6 and 50.1%, and 3.7, 12.6 and 56.4%, respectively. This result shows that the XP-A protein recognizes the DNA damage induced by acetaldehyde.

## DISCUSSION

Acetaldehyde induces GG to TT (or CC to AA) tandem mutations in double-stranded shuttle vectors. It is difficult to imagine DNA lesions that induce tandem mutations except by way of intra-strand crosslinks. UV light induces CC to TT (17,18), and *cis*-diamminedichloroplatinum(II) induces GG to TT tandem base substitutions (16). It is well known that UV light induces cytosine dimers and *cis*-diamminedichloroplatinum(II) induces G–G intra-strand crosslinks (19). Metal-induced oxygen radicals also induce GG to AA tandem mutations (20) and are believed to induce intra-strand crosslinks (21). Our results show that acetaldehyde forms intra-strand crosslinks in adjacent guanine bases. Adenines would be incorporated at the opposite sites of

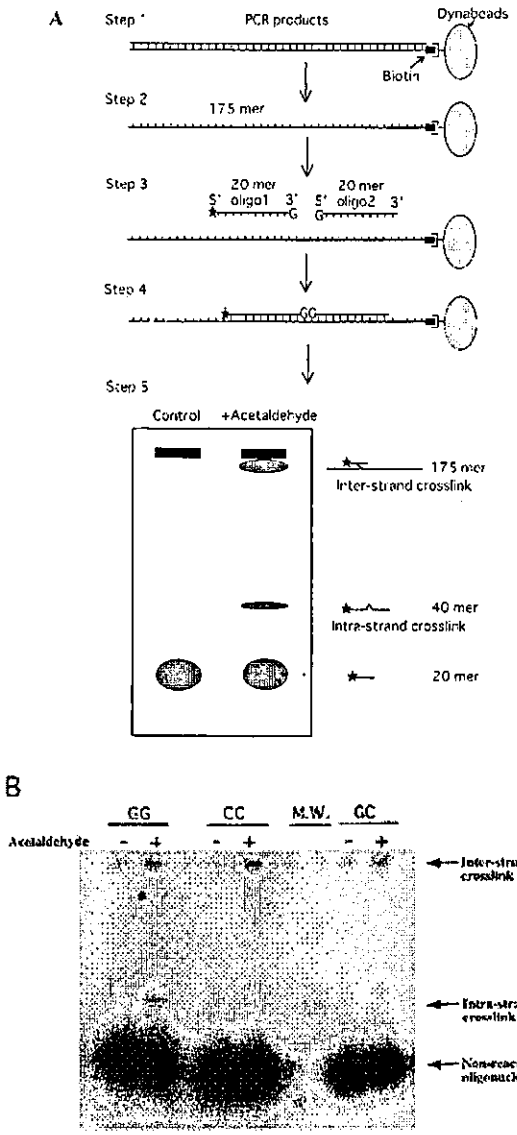


**Figure 3.** (A) Scheme of crosslink assay. The sequences of oligonucleotides used in this assay are as follows: primer 1, d(TTAACGCGAATTTTAACAAA) (biotinylated); primer 2, d(TCGTGACTGGGAAAACCCTG); oligo 1, d(TCGTGACTGGGAAAACCCTG); oligo 2, d(GCGTTACCCAACTTAATCGC); oligo 3, d(GCGTTACCCAACTTAATCGC); oligo 4, d(CCTTGCAGCACATCCCCCTT); oligo 5, d(GGCGTTACCCAACTTAATCG); oligo 6, d(CTTGCAGCACATCCCCCTTT). Step 1: the 175 bp region of pBluescript KS(−) was amplified by PCR using primer 1 and 2, and the PCR products were bound to Dynabeads. Step 2: the Dynabeads were washed with NaOH to make the 175mer single-stranded DNA. Step 3: the $^{32}$P-labeled oligo 1 and non-labeled oligo 2 were annealed with the 175mer single-stranded DNA for detecting intra-strand crosslinks between adjacent guanine bases. Alternatively, the $^{32}$P-labeled oligo 3 and non-labeled oligo 4, or the $^{32}$P-labeled oligo 5 and non-labeled oligo 6, were also annealed to detect CC- or GC-intra-strand crosslinks, respectively. Step 4: the substrates were treated with acetaldehyde. Step 5: the treated substrates were subjected to electrophoresis on 12% polyacrylamide gel (50% urea, 1× TBE) and the gel was autoradiographed. (B) Result of the crosslink assay. The substrates that were designated to detect intra-strand crosslinks between adjacent guanine bases (GG), adjacent cytosine bases (CC)and adjacent guanine and cytosine bases (GC) were treated with or without 2 M acetaldehyde for 48 h at 4°C and were subjected to the denatured gel electrophoresis. $^{32}$P-labeled 40mer oligonucleotide was also used as a molecular weight maker (M.W.).

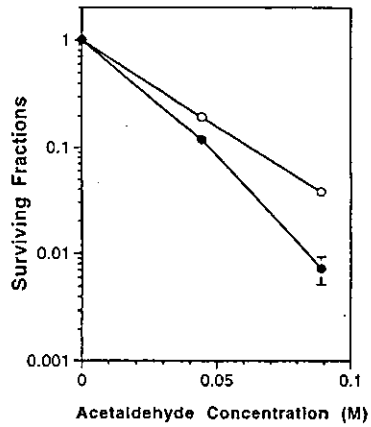


**Figure 4.** Survival curves of normal (VA13 ) (○) and XP-A [XP2OS(SV)] (●) cells treated with acetaldehyde. Three plates were used for each data point and the error bar represents standard deviation. Except for one point, the error bars were too small to show.

crosslinked guanines at DNA replication, which resulted in GG to TT tandem base substitutions. The chemical structure of this crosslink is still unknown. Chaw *et al.* showed that formaldehyde forms (-NH-$CH_2$-NH-) crosslinks between G–G, G–C, A–C, A–G and A–A (22). Acetaldehyde should form DNA crosslinks by a similar mechanism to formaldehyde, i.e. it should form covalent bridges between amino groups of DNA bases. Cytosine and adenine, as well as guanine, have amino groups in their molecules. Although we could not detect crosslinks at a 5′-GC-3′ site in our assay system, a little crosslink must be formed at this site, which leads to tandem mutations at 5′-GC-3′ sites. In single-stranded shuttle vectors, different from in double-stranded vectors, acetaldehyde does not induce GG tandem mutations, but induces GC tandem mutations. The types of GC tandem mutation are also different. We have no clear explanation of these observations, but it may depend on the difference of (i) the three-dimensional structure, (ii) DNA replication mechanisms and (iii) DNA repair mechanisms, between single- and double-stranded shuttle vectors.

Acetaldehyde is commonly present in many organisms. Therefore, it is not surprising that organisms have repair pathways for acetaldehyde-induced DNA damage. Results from the cell survival, shuttle vector mutagenesis and XP-A protein-binding assays strongly suggest that the human nucleotide excision repair system is involved in the repair of the acetaldehyde-induced DNA damage. In the cell survival assay, XP cells were slightly sensitive to acetaldehyde compared with normal cells, but the difference of sensitivity was not as distinct between the two cell lines. The reason should be that DNA damage is not the only biological lesion induced by acetaldehyde. Since acetaldehyde is reactive with the amino residue, it may react with proteins, amino acids and RNA molecules, as well as DNA molecules.

Since treatment with acetaldehyde produces very specific base changes in DNA, these changes can be used as a probe to show acetaldehyde as a causal agent in human tumors. The majority of human cancers have point mutations in the *p53* tumor suppressor gene (23), and the specificity in the types of mutations in this gene may be related to causal environmental agents; e.g. the CC to TT tandem double mutations in skin tumors to UV sunlight (17,18,24,25), and the G to T transversions in liver tumors to aflatoxinB1 (26,27). The database of *p53* gene somatic mutations

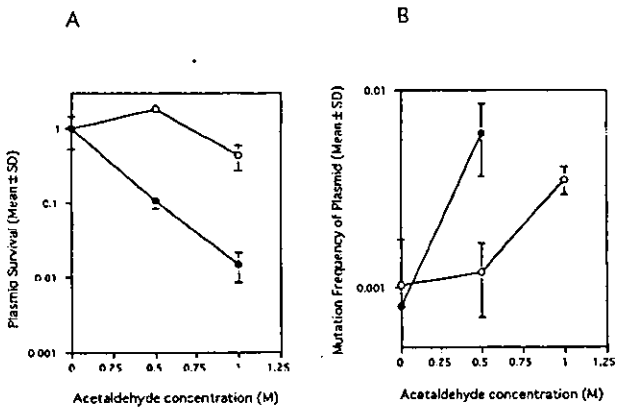


Figure 5. (A) Survival of acetaldehyde-treated pMY189 replicated in normal (VA13) (○) and XP-A [XP2OS(SV)] (●) cell lines. The relative number of ampicillin-resistant bacterial colonies obtained after repair and replication of acetaldehyde-treated pMY189 in the cells followed by transformation of the indicator *E.coli* is shown. (B) Mutation of acetaldehyde-treated pMY189 replicated in normal (VA13; ○) and XP-A [XP2OS(SV); •] cell lines. The ratio of nalidixic acid-resistant bacterial colonies versus total bacterial colonies, obtained after repair and replication of acetaldehyde-treated pMY189 in the cells followed by transformation of the indicator *E.coli*, is shown. The data show mean values from three independent transfection experiments for each cell line, and the error bar represents the standard deviation.

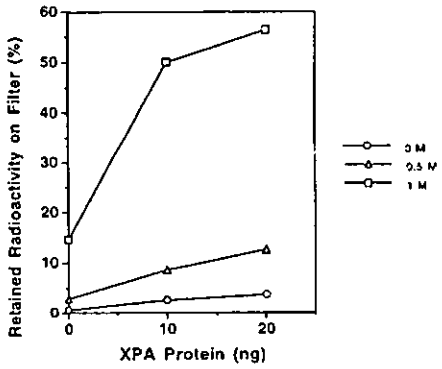


Figure 6. XP-A protein binding assay to acetaldehyde treated DNA. One ng of $^{32}$P-labeled DNA, either untreated (○), acetaldehyde-treated at 37°C for 1 h with a concentration of 0.5 M (Δ) or 1 M (□), was incubated with purified XP-A protein in the presence of excess amount of BSA (5 µg). DNA bound to protein was collected on nitrocellulose filters.

in human tumors and tumor cell lines (28) was searched. Of 4496 mutations in the *p53* gene in the database, only three GG to TT (or CC to AA) tandem base substitutions were found. Five GC to TT (or GC to AA) and three GG to AT (or CC to AT) tandem base substitutions were also found in 4496 mutations. Five of these tandem base substitutions were found in the respiratory tract cancers and one was found in a stomach cancer. Although no details of the smoking and drinking histories of the subjects concerned were given, these mutations may be related to smoking or alcohol consumption. A recent finding indicates that human aldehyde dehydrogenase gene (*ALDH2*) genotype is related to esophageal cancer risk (29). A study of the relationship between the tandem base substitutions in esophageal tumors and epidemiological and genetic properties of the patients, such as smoking and drinking habits and *ALDH2* genotypes, may reveal the significance of acetaldehyde on the development of human tumors.

## ACKNOWLEDGEMENTS

We thank Dr H.Asahina for technical advice on the XP-A protein binding assay. M.K. was supported by a fellowship from the Japan Society for the Promotion of Science. This work was supported in part by The Japanese Ministry of Education, Science, Sports and Culture (Grant in Aid for Scientific Research 08555137). Preliminary reports of these studies were presented in October 1996 in Yokohama at the 55th annual meeting of the Japanese Cancer Association.

## REFERENCES

1 Dellarco, V. L. (1988) *Mutat. Res.* **195**, 1–20.
2 IARC (1985) *IARC Monographs on the Evaluation of Carcinogenic Risk of Chemicals to Humans: Allyl Compounds, Aldehydes, Epoxides and Peroxides*. International Agency for Research on Cancer, Lyon, France.
3 IARC (1985) *IARC Monographs on the Evaluation of Carcinogenic Risk of Chemicals to Humans: Tobacco Smoking*. International Agency for Research on Cancer, Lyon, France.
4 Ristow, H. and Obe, G. (1978) *Mutat. Res.* **58**, 115–119.
5 Obe, G., Natarajan, A. T., Meyers, M. and Hertog, A. D. (1979) *Mutat. Res.* **68**, 291–294.
6 Korte, A. and Obe, G. (1981) *Mutat. Res.* **88**, 389–395.
7 He, S. M. and Lambert, B. (1985) *Mutat. Res.* **158**, 201–208.
8 Bariliak, I. R. and Kozachuk, S. Y. (1983) *Tsitol. Genet. (Russian)* **17**, 57–60.
9 Grafström, R. C., Dypbukt, J. M., Sundqvist, K., Atzori, L., Nielsen, I., Curren, R. D. and Harris, C. C. (1994) *Carcinogenesis* **15**, 985–990.
10 Vaca, C. E., Fang, J. L. and Schweda, E. K. H. (1995) *Chem. Biol. Interact.* **98**, 51–67.
11 Fang, J. L. and Vaca, C. E. (1997) *Carcinogenesis* **18**, 627–632.
12 Matsuda, T., Yagi, T., Kawanishi, M., Matsui, S. and Takebe, H. (1995) *Carcinogenesis* **16**, 2389–2394.
13 Akasaka, S., Takimoto, K., Yamamoto, K. (1992) *Mol. Gen. Genet.* **235**, 173–178.
14 Robins, P., Jones, C. J., Biggerstaff, M., Lindahl, T. and Wood. R. D. (1991) *EMBO J.* **10**, 3913–3921.
15 Armitage, P. (1971) *Statistical Methods in Medical Research*. J. Wiley and Sons, New York.
16 Bubley, G. J., Ashburner, B. P. and Teicher, B. A. (1991) *Mol. Carcinogen.* **4**, 397–406.
17 Yagi, T., Tatsumi-Miyajima, J., Sato, M., Kraemer, K. H. and Takebe, H. (1991) *Cancer Res.* **51**, 3177–3182.
18 Drobetsky, E. A., Grosovsky, A. J. and Glickman, B. W. (1987) *Proc. Natl. Acad. Sci. USA* **84**, 9103–9107.
19 Friedberg, E. C., Walker, G. C. and Siede, W. (1995) *DNA Repair and Mutagenesis*, ASM press, Washington, DC, pp 34.
20 Reid, T. M., Feig, D. I. and Loeb, L. A. (1994) *Environ. Health. Perspect.* **102** (Suppl 3), 57–61.
21 Randerath, K., Randerath, E., Smith, C. V. and Chang, J. (1996) *Chem. Res. Toxicol.* **9**, 247–254.
22 Chaw, Y. F. M., Crane, L. E., Lange, P. and Shapiro, R. (1980) *Biochemistry* **19**, 5525–5531.
23 Harris, C. C. and Hollstein, M. (1993) *N. Engl. J. Med.* **329**, 1318–1327.
24 Brash, D. E., Rudolph, J. A., Simon, J. A., Lin, A., Mckenna, G. J., Baden, H. P., Halperin, A. J. and Ponten, J. (1991) *Proc. Natl. Acad. Sci. USA* **88**, 10124–10128.
25 Sato, M., Nishigori, C., Zghal, M., Yagi, T. and Takebe, H. (1993) *Cancer Res.* **53**, 2944–2946.
26 Levy, D. D., Groopman, J. D., Lim, S. E., Seidman, M. M. and Kraemer, K. H. (1992) *Cancer Res.* **52**, 5668–5673.
27 Bressac, B., Kew, M., Wands, J. and Ozturk, M. (1991) *Nature* **350**, 429–431.
28 Hollstein, M., Rice, K., Greenblatt, M. S., Soussi, T., Fuchs, R., Sorlie, T., Hovig, E., Smith-Sorensen, B., Montesano, R. and Harris, C. C. (1994) *Nucleic Acids Res.* **22**, 3551–3555.
29 Holi, H., Miyake, S., Yoshino, K., Endo, M. and Yuasa, Y. (1997) *J. Clin. Gastroenterol.*, **25**, 568–575.

Carcinogenesis vol.16 no.10 pp.2389–2394, 1995

# Molecular analysis of mutations induced by 2-chloroacetaldehyde, the ultimate carcinogenic form of vinyl chloride, in human cells using shuttle vectors

**Tomonari Matsuda, Takashi Yagi[1], Masanobu Kawanishi, Saburo Matsui and Hiraku Takebe[1,2]**

Center for Environmental Quality Control, Kyoto University, 1-2 Yumihama, Otsu, Shiga 520 and [1]Department of Radiation Genetics, Faculty of Medicine, Kyoto University, Yoshida-konoe-cho, Sakyo-ku, Kyoto 606-01, Japan

[2]To whom correspondence should be addressed

**Vinyl chloride (VC) is a carcinogen associated with human and animal cancers. The ultimate carcinogenic form of VC, 2-chloroacetaldehyde (CAA), has been suspected to be mutagenic and we confirmed the mutagenicity of CAA using a modified shuttle vector plasmid. Base sequence analyses of 109 mutant plasmids with mutations in the *supF* gene, which were treated with CAA and propagated in the cultured human cells, revealed that more than half of the single base substitutions were G:C to A:T transitions with eight hotspots. The majority of the mutations involving G:C base pairs were in 5′-AAGG-3′ or 5′-CCTT-3′ sequences suggesting that these sequences are the main targets of mutagenesis caused by CAA.**

## Introduction

Vinyl chloride (VC*) is one of the widely used raw materials in the polymer industries. Many epidemiological studies and case reports have demonstrated that VC is associated with cancers in liver, brain, lung and the haematolymphopoietic system. The IARC working group classified VC as belonging to Group 1, which represents the substances with carcinogenicity supported by sufficient evidence in humans and animals (1,2).

Vinyl chloride is metabolized by the cytochrome P450-dependent monooxygenases to 2-chloroethylene oxide and then rapidly converted to 2-chloroacetaldehyde (CAA) in mammalian livers (3). 2-Chloroacetaldehyde reacts with DNA bases *in vitro*, resulting in production of four known cyclic adducts: 1,$N^6$-ethenoadenine (εA), 3,$N^4$-ethenocytosine (εC), $N^2$,3-ethenoguanine ($N^2$,3-εG) and 1,$N^2$-ethenoguanine (1,$N^2$-εG) (4). These cyclic adducts were detected in liver DNA in rats following exposure to VC (5,6) and have been shown to cause mutations (7–13).

Recently, mutations involving G:C to A:T transitions in the second nucleotide at codon 13 in the c-Ki-*ras*-2 gene were detected in liver angiosarcomas in VC plant workers (14). This type of mutation could be specific to VC since the same type of mutation was found in bacteria exposed to VC (9–13,15). We intend to confirm whether this VC specific mutation arises in human cells.

The shuttle vector plasmid, pZ189 (16) and its derivative pS189 (17) and pYZ289 (18) have been widely used in assessing the carcinogen-induced mutations in mammalian cells. Each type of the plasmid carries a bacterial suppressor tRNA gene, *supF*, as a target gene for mutagenesis. The *supF* gene is small enough (176 base pairs) to facilitate rapid sequence analysis in many samples. We constructed a new shuttle vector plasmid, pMY189, by modification of the plasmid pZ189 to make the plasmid sequence suitable for the fluorescence dye primer cycle sequencing method.

We treated the shuttle vector plasmid pMY189 with CAA, the ultimate carcinogenic form of VC and transfected the plasmids to human fibroblast cells. The plasmids containing mutations in the *supF* gene were detected with the indicator bacteria system developed by Akasaka *et al.* (19) and the mutations were analyzed by the automatic DNA sequencing.

*Abbreviations: VC, vinyl chloride; CAA, 2-chloroacetaldehyde; IPTG, isopropyl-β-D-thiogalactoside; X-gal, 5-bromo-4-chloro-3-indoyl-β-D-galactoside; PBS, phosphate buffered saline.

## Materials and methods

### *Chemicals*

2-Chloroacetaldehyde, ampicillin, chloramphenicol, nalidixic acid, isopropyl-β-D-thiogalactoside (IPTG) and 5-bromo-4-chloro-3-indoyl-β-D-galactoside (X-gal) were obtained from Wako Chemicals (Osaka, Japan). Restriction endonucleases and other enzymes were obtained from Takara Shuzo (Kyoto, Japan). QIAGEN plasmid-kit and Wizard™ Minipreps DNA Purification Systems were purchased from QIAGEN Inc. (Chatsworth, CA) and Promega (Madison, WI) respectively.

### *Cells*

SV40-transformed human fibroblast cell lines were used. A normal human cell line WI38-VA13 (20) was obtained from the American Type Culture Collection (Rockville, MD). DNA repair deficient XP2OS(SV) cells were previously established by us from a Japanese group A XP patient (21). All cells were cultured in Dulbecco's modified minimum essential medium (Nikken, Kyoto, Japan) supplemented with 10% fetal bovine serum (Hyclone, Logan, UT).

### *Plasmid construction*

The shuttle vector plasmid pZ189 was modified to be directly applied to the dye primer cycle sequencing method followed by the automatic DNA sequencing by a 370A DNA sequencer (Applied Biosystems, Foster, CA). Two 42-mer oligonucleotides were synthesized by a 380B DNA synthesizer (Applied Biosystems). One contains the sequence of the −21M13 fluorescent dye-labelled universal primer (5′-TGTAAAACGACGGCCAGT-3′) which is commercially available (Applied Biosystems) (5′-GACGAATTCTGTAAAA-CGACGGCCAGTGAGCTCGAATTCTTG-3′). The other is its complementary sequence, (5′-CAAGAATTCGAGCTCACTGGCCGTCGTTTTACAGAAT-TCGTC-3′). Both oligomers contain *Eco*RI restriction sequences (5′-GAATTC-3′) at their 5′- and 3′- ends and a *Sac*I restriction sequence (5′-GAGCTC-3′). Twenty micrograms each of these oligomers were annealed by heating and cooling in a solution of 750 mM NaCl and 75 mM $Na_3$ citrate. After ethanol precipitation, the annealed fraction (double strand DNA) was digested with *Eco*RI and inserted into the *Eco*RI site of pZ189 with T4 DNA ligase. The direction of the inserted oligomer was confirmed by the *Sac*I digestion and the DNA sequencing. The modified pZ189 was named pMY189 (Figure 1).

### *Bacterial strains*

The indicator *Escherichia coli* strain KS40/pKY241 (19) was kindly supplied from Dr S.Akasaka, Division of Industrial Health, Osaka Prefectural Institute of Public Health, Osaka, Japan. KS40 is a nalidixic acid-resistant (*gyrA*) derivative of MBM7070 [*lacZ* (am) *CA7070 lacY1 HsdR HsdM* Δ (*araABC-leu*)*7679 galU galK rpsL thi*] (22), which has been used for detection of the mutated pZ189. Plasmid pKY241 was constructed by Akasaka *et al.* (19) and contains a chloramphenicol resistant marker and a *gyrA* (amber) gene. *Escherichia coli* KS40/pKY241 cells carrying the active *supF* gene are sensitive to nalidixic acid, whereas the cells carrying the mutated *supF* form colonies on plates containing nalidixic acid, chloramphenicol and ampicillin. To ensure the selection of the mutated *supF* gene, IPTG and X-gal were

added to the selection plates. *Escherichia coli* cells containing the active *supF* gene produce blue colonies, whereas cells having the mutated *supF* gene produce white or light blue colonies.

*Treatment of plasmids with CAA and transfection to human cells*

Purified stocks of pMY189 were prepared by using the QIAGEN plasmid purification kit. The plasmids (40 μg) were treated with various concentrations of CAA in 0.3 M sodium acetate in total volume of 0.5 ml. The reaction was allowed to proceed for 1 h at 37°C followed by ethanol precipitation of the plasmids to remove the nonreacted excess CAA and the plasmids were redissolved in 0.5 ml of TE buffer (pH 8).

The human cells, WI38-VA13 or XP2OS (SV) were trypsinized, washed and suspended in Dulbecco's phosphate-buffered saline (PBS) solution (pH 7.5). Cells ($2\times10^7$) plus 14.4 μg CAA-treated pMY189 in PBS solution (0.2 ml) were placed in an electroporation chamber (electrodes 0.3 cm apart) (PDS Inc. Madison, WI) and the cells were transfected with the plasmids by electric pulses (600 V, 5×). The cells were plated in five 10 cm dishes and incubated at 37°C for 72 h in a $CO_2$ incubator.

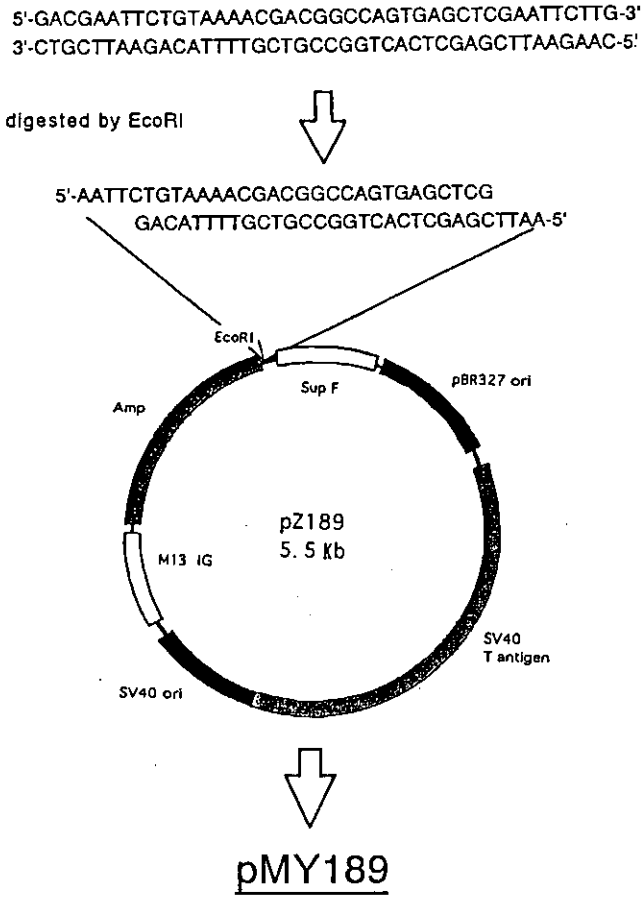


**Fig. 1.** Construction and the structure of the shuttle vector plasmid pMY189. Two 42 mer oligonucleotides, one of them containing a sequence of −21M13 5'-fluorescent dye-labelled universal primer for the automatic DNA sequencing, were annealed and digested by *Eco*RI, and ligated into the *Eco*RI site of the pZ189.

*Plasmid recovery, selection of mutated supF and DNA sequencing*

Plasmids were extracted from the cells using Wizard™ Minipreps DNA Purification Systems (Promega, Madison, WI). The purified plasmids were digested with the restriction endonuclease *Dpn*I (Boehringer-Yamanouchi, Tokyo, Japan) to eliminate the nonreplicated plasmids which retain the bacterial methylation pattern.

Plasmid DNA was introduced into the indicator bacteria KS40/pKY241 by the electroporation apparatus *E.coli* Pulser (Biorad, CA). The bacterial cells were plated in LB agar containing nalidixic acid, ampicillin, chloramphenicol at concentrations of 50, 150 and 30 μg/ml respectively, supplemented with IPTG and X-gal to select the plasmids containing the mutated *supF* genes. A part of the cells was plated on LB agar containing ampicillin and chloramphenicol to measure the total number of transformants. After 24 h incubation at 37°C, colonies were counted and mutation frequencies were calculated.

Mutated plasmids were extracted and purified from the overnight culture with the Wizard Minipreps Purification System (Promega) and the base sequences of the *supF* gene of the plasmids were determined with the −21M13 primer and Dye-Primer Cycle Sequencing Reagent Kit using a 370A automatic DNA sequencer (Applied Biosystems).

## Results

### *Plasmid mutagenesis*

2-Chloroacetaldehyde treatment of the pMY189 plasmids increased the frequency of mutation in the *supF* gene in both repair-proficient and repair-deficient cells (Table I). The background plasmid mutation frequency was 2.2 and $1.4\times10^{-4}$ with VA13 and XP-A cells respectively. The mutation frequency increased similarly in both cell lines following treatment of the plasmid with CAA; and ~7- and 40-fold increases with 0.13 and 0.51 M CAA respectively, were observed.

### *Base sequence analysis*

Analysis of 109 *supF* mutant plasmids transfected to the repair proficient cells was carried out by the nucleotide sequencing. Base sequence changes in plasmids were classified as single base substitutions, tandem base substitutions, multiple base substitutions (2 ≤ base substitutions more than three bases apart), frameshifts (single base insertions or deletions) and large deletions (Table II). Large deletions (average deleted sequence, 113 base pairs; range, 26–184 base pairs) were found in 10% of the plasmids and 14% of the plasmids contained the multiple base substitutions. The tandem base substitutions and the frameshift mutations were scarce. The rest (72%) contained the single base substitutions.

Among the mutant plasmids with single base substitutions, 90% were the substitutions of G:C base pair (Table III). The most frequent type of the base substitution mutations was G:C to A:T transition (54%). Other types of the base substitutions

**Table I.** Mutation frequency of CAA-treated plasmids pMY189 propagated in normal or xeroderma pigmentosum fibroblasts

| Concentration of CAA (M) | WI38-VA13 | | | XP2OS(SV) | | |
|---|---|---|---|---|---|---|
| | No. of colonies | | | No. of colonies | | |
| | Mutant | Total (× $10^4$) | Mutation frequency (× $10^{-4}$) | Mutant | Total (× $10^4$) | Mutation frequency (× $10^{-4}$) |
| 0 | 85 ± 7.1 | 38.0 | 2.2 ± 0.2 | 2.3 ± 1.9 | 1.6 | 1.4 ± 1.2 |
| 0.13 | 151.3 ± 11.9 | 10.2 | 14.9 ± 1.2 | 160.7 ± 18.3 | 12.1 | 13.3 ± 1.5 |
| 0.26 | | | | 241.0 ± 23.8 | 7.7 | 31.4 ± 3.1 |
| 0.51 | 989.0 ± 61.7 | 16.7 | 59.2 ± 3.7 | 154.0 ± 4.5 | 2.8 | 55.3 ± 1.6 |

Average colony numbers from three independent experiments are given with the standard error of the mean.

were G:C to T:A transversion (30%), G:C to C:G transversion (6%), A:T to G:C transition (9%) and A:T to T:A transversion (1%). No single base A:T to C:G transversion was detected. Figure 2A shows the targets of the single base substitutions in the *supF* gene, compiled from the previous reports (16,17,23–39). Among the reported 93 target sites (* in Figure 2A), 54 sites are present in G:C base pairs and 39 sites are present in A:T base pairs. The proportion of the base substitution at G:C base pairs is higher than that at A:T base pairs, even when the difference of the number of target sites between G:C and A:T base pairs is adjusted (Table III).

*Mutation spectra*

Distribution of the single base substitutions and tandem or multiple base substitutions in the *supF* gene with the repair proficient cell is also shown in Figure 2A. Eight sites (123,133,134,156,159,160,168 and 169) had four or more single base substitutions. Most of the single base substitutions (91%) were produced at these hotspots. Seven of the eight hotspots were located at G:C base pairs. Five G:C to A:T or G:C to T:A hotspots (123,159,160,168 and 169) are located at G:C base pairs in 5′-AAGG-3′ sequences.

All multiple base substitutions were found in separate positions, except one tandem base substitution (Figure 2B). There are 15 two-base substitutions and one three-base substitutions.

## Discussion

Plasmids pMY189 treated with CAA yielded the same frequency of mutations when they were propagated in XP-A and normal cells, suggesting that the DNA damage induced by CAA is not repaired by the nucleotide excision repair pathway in human cells. This was supported by the preliminary experiment indicating that the survival of the CAA-treated pMY189 plasmids introduced in *E.coli* MBM7070 (wild type) and KY46 (uvrA) were the same (data not shown).

CAA-induced DNA adducts were reported to be repaired by a human 3-methyladenine DNA glycosylase (40,41), suggesting that DNA repair other than the nucleotide excision type may be involved.

In mutation spectra of the single base substitutions, 72 out of 78 (92%) were located in the eight mutational hotspots among 93 mutation target sites in the *supF* gene. There are four 5′-AAGG-3′ or 5′-CCTT-3′ sequences in the *supF* gene (positions 68–71, 120–123, 157–160 and 168–171). Fifty-seven out of 78 (73%) single base substitutions were located at G:C pairs in these 5′-AAGG-3′ or 5′-CCTT-3′ sequences. This suggests that G:C pairs in the 5′-AAGG-3′ or 5′-CCTT-3′ sequences are the major mutational targets by CAA. The sequence 5′-AAGG-3′ on position 68–71 was not mutated. However, no mutation at position 70 and only two mutations at position 71 have been reported previously, suggesting that these sites are phenotypically silent or may be protected from attack by the chemical caused by the secondary structure of the gene. The possibility that we isolated sibling mutants is unlikely, because we took 109 colonies out of about 3000 mutant colonies and no identical mutation was found in the tandem and multiple base substitutions, frameshifts and deletion mutations. We do not know why such a high sequence specificity is achieved. DNA damage may be induced or DNA repair may be blocked selectively on this sequence by unknown mechanisms.

G:C to A:T transition mutations are predominant (53.8%), supporting the previous findings that chloroethylene oxide-treated *E.coli* (15) and CAA-treated gapped duplex M13 DNA (13) had mainly G:C to A:T transitions. The adducts which can cause mutations in G:C base pairs could be the 3,$N^4$ ethenocytosine (εC) and the $N^2$,3-ethenoguanine ($N^2$,3-εG). The $N^2$,3-εG:T mismatch caused G:C to A:T transitions in an *in vitro* DNA replication experiment (8). Site specifically incorporated $N^2$,3-εG in the M13 double strand DNA resulted in G to A transitions (11) and site specifically incorporated εC in the M13 single strand DNA (9) or gapped duplex DNA (10,12) led mainly to C to T transitions. These reports and our experiment suggest that the major contributors to the G:C to A:T transitions induced by CAA in human cells are εC and $N^2$,3-εG.

The previously published data of the mutations in G:C base pairs induced by CAA or its related cyclic adducts are summarized in Table IV. Compared with other studies using M13 phage, our results show relatively high frequency of G:C to T:A transversion mutations. It may reflect the different mechanisms of the DNA repair or the mutation fixation in *E.coli* and human cells, since the similar difference was observed in UV-induced mutations in M13 and human cells (33,42).

The published data of the mutations in A:T base pairs induced by CAA or its related cyclic adducts are summarized in Table V. The predominance of A:T to G:C transition mutations in our data supported the previous findings that site-specifically incorporated εA and 4-amino-5-(imidazole-2-yl)imidazole (β) in single strand M13 DNA induced mainly A:T to G:C transitions (9) in *E.coli*. The data of mutations in the CAA-treated M13 gapped duplex DNA replicated in *E.coli*, however, showed the predominance of A:T to T:A transversions (13). In addition to the difference in the mechanism of the

**Table II.** Types of mutations in the *supF* gene in CAA-treated shuttle vector plasmids pMY189 propagated in human fibroblast cells WI38-VA13

| Type of mutation | No. | Percentage of total |
|---|---|---|
| *Base substitution* | | |
| Single base substitution | 78 | 71.6 |
| Tandem base substitution | 1 | 0.9 |
| Multiple base substitution | 15 | 13.8 |
| *Frameshift* | | |
| Single base insertion | 0 | 0.0 |
| Single base deletion | 1 | 0.9 |
| Deletion over 3 base pair | 12 | 10.1 |
| Others | 2 | 1.8 |
| Total | 109 | 100 |

**Table III.** Types of CAA-induced single base substitutions in the *supF* gene in shuttle vector plasmids pMY189 propagated in human fibroblast cells WI38-VA13

| Type of mutation | No. (%) of mutants | No. of mutants/target site[a] (%) |
|---|---|---|
| G:C to A:T | 42 (53.8) | 0.778 (51.8) |
| G:C to T:A | 23 (29.5) | 0.426 (28.4) |
| G:C to C:G | 5 (6.4) | 0.093 (6.2) |
| A:T to G:C | 7 (9.0) | 0.179 (11.9) |
| A:T to T:A | 1 (1.4) | 0.026 (1.7) |
| A:T to C:G | 0 (0.0) | 0 (0.0) |
| Total | 78 (100) | 1.502 (100) |

[a]Numbers of targets of the single base substitution mutations in the *supF* gene are 54 at G:C pairs and 39 at A:T pairs.

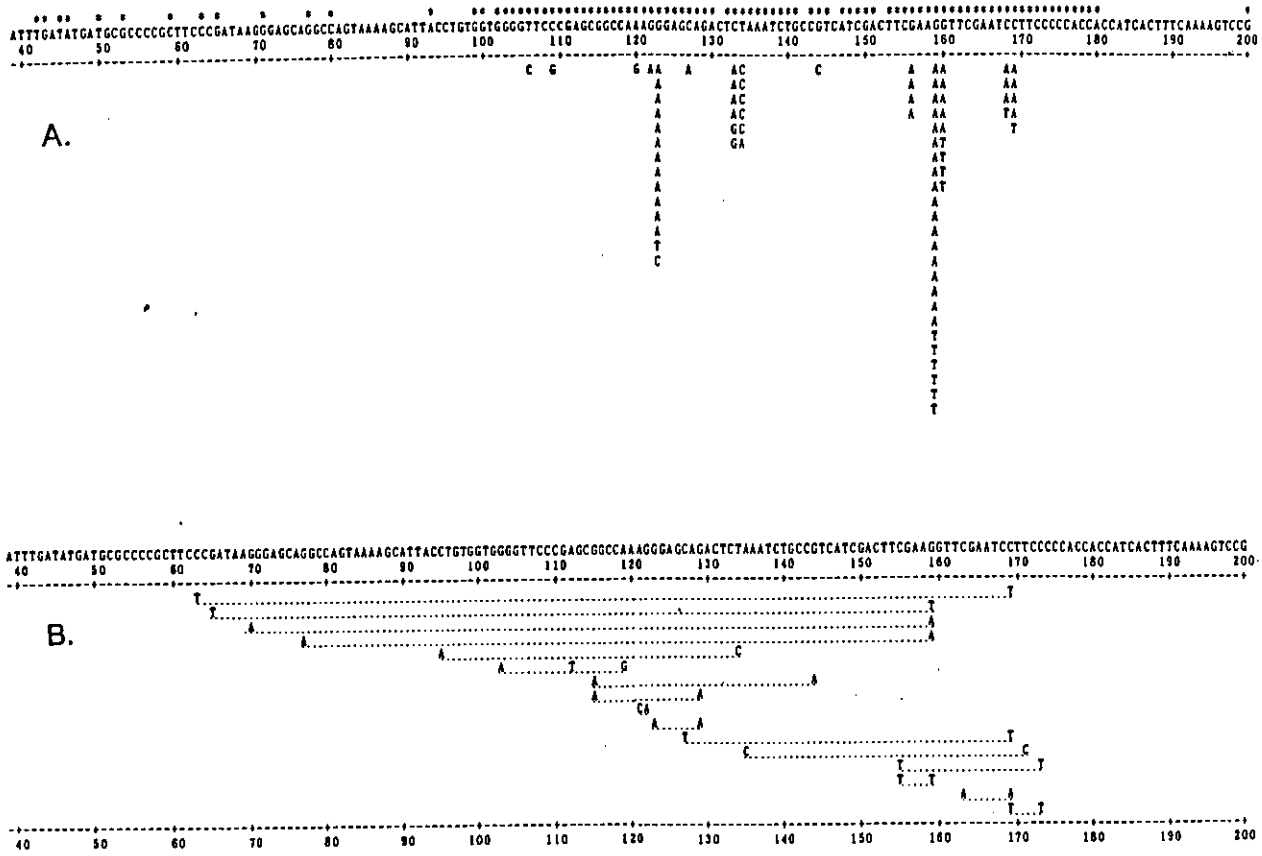


**Fig. 2.** Locations of the single (A) and tandem and multiple (B) base substitution mutations found in the *supF* suppressor tRNA gene in CAA-treated plasmids pMY189 propagated in WI38-VA13 cells. Each letter under the sequence represents a single base substitution mutation found in an independent plasmid (A). Multiple base substitutions are shown in (B). Positions of the targets of the single base substitutions which inactivate the suppressor function are as follows [Position (Ref.)]: 42(16), 43(16,39), 45(16), 46(16), 50(16, 38), 53(28), 59(39), 62(39), 63(16), 65(16,24,26), 71(16,26), 77(16,31), 80(24), 93(24,26), 99(24,26,34), 100(16), 102(16,17,25), 103(16,17,37), 104(16,17,33,37), 105(16,17,37,33,38), 106(16,34,38), 107(37), 108(16,23,26,31,36–39), 109(16,17,24–26,29,31,33,34,37), 100(16,25,30,31,36), 111(16,23,26,30,37), 112(16,17,29,30,33,34,37,38), 113(16,17,23,25,26,31,34,37,38), 114(16,26), 115(16,17,25,29,37,38), 116(16,17,25,26,29,31), 117(16,36), 118(16,24,34), 119(16,34), 120(16,24,31,33–35,37,38), 121(27,37), 122(16,25,31,34,36,37), 123(16,17,23–26,32–34,37–39), 124(16,17,24,33,34,36,38,39), 125(16,37), 126(16,37), 127(16,17,25,29,33,34,37,38), 128(30), 129(16,17,24–26,31,32,34,35), 130(37), 132(16,34,37), 133(16,17,24–27,29,31–34,38), 134(16,27,31,33,34,37–39), 135(16,27,31,33–35,38,39), 136(16,17,24,26,27,29,31,33–37,39), 137(16,17,31,33,34), 138(37), 139(16,17,24–26,29,33–35,37,38), 140(16,24,25,30,34), 141(16,25,33,34,37,38), 143(16,25), 144(16,17,24,26,29,33,34,37), 145(37), 147(35), 148(Akasaka *et al.*, in press), 149(26,33,35), 150(16,31,37), 151(37), 153(37,39), 154(16,31,35,37), 155(16,17,23,25,26,29,31–37,39), 156(16,17,23–26,31–39), 157(37), 158(16,31,34,37), 159(16,17,23–26,29,31–39), 160(16,17,23–27,29,30,31,33,34,38), 161(16,27,33,34,37), 162(16,25,27,34,36,37), 163(16,31,32,37), 164(16,17,24–26,29,31,33,34,36,37,39), 165(16,25,31,33,34,36,37), 166(27,37), 167(16,37), 168(16,17,23–27, 29–39), 169(16,17,23–26,29–31,33–39), 170(37), 171(16,34,37,39), 172(16,17,24–26,29,33,34,37,38), 173(16,34,39), 174(16,17,25,37), 175(16,31,33,37), 176(17), 177(16,17,34,35), 178(17,25), 179(16,34), 180(37), 200(16).

**Table IV.** Types of G:C base substitution mutations induced by 2-chloroacetaldehyde and its related cyclic adducts

| Type of mutation | No. (%) of mutants | | | | |
|---|---|---|---|---|---|
| | εG[a] M13 dsDNA in *E.coli* | εC[b] M13 ssDNA in *E.coli* | εC[c] M13 gdDNA in *E.coli* | CAA treated[d] M13 gdDNA in *E.coli* | Our data[e] |
| G:C to A:T | 134 (99.3) | 31 (56.4) | (64.0) | 80 (72.1) | 63 (64.9) |
| G:C to T:A | 0 (0) | 12 (21.8) | (10.9) | 20 (18.0) | 29 (29.9) |
| G:C to C:G | 1 (0.7) | 0 (0) | (0) | 11 (9.9) | 5 (5.2) |
| 1 base deletion | 0 (0) | 12 (21.8) | (25.0) | 0 (0) | 0 (0) |
| Total | 135 (100%) | 55 (100%) | (100%) | 111 (100%) | 97(100%) |

[a]Site-specifically incorporated $N^2$,3-ethenoguanine (5′-GG(εG)AAA-3′) in double strand M13DNA was replicated in *E.coli* cells (11).
[b]Site-specifically incorporated 3,$N^4$-ethenocytosine (5′-TAG(εC)GGG-3′) in single strand M13DNA was replicated in *E.coli* cells (9).
[c]Site-specifically incorporated 3,$N^4$-ethenocytosine (5′-TT(εC)TT-3′) in gapped duplex M13DNA was replicated in *E.coli* cells (10). Mutation was analyzed by the multiplex sequence analysis.
[d]The CAA treated gapped duplex M13DNA was replicated in UV-irradiated *E.coli* cells (13).
[e]Data contain all single, tandem and multiple base substitutions.

Table V. Types of A:T base substitution mutations induced by 2-chloroacetaldehyde (CAA) and its related cyclic adducts

| Type of mutation | No. (%) of mutants | | | |
|---|---|---|---|---|
| | εA[a] M13 ssDNA in *E.coli* | β[b] M13 ssDNA in *E.coli* | CAA treated[c] M13 gdDNA in *E.coli* | Our data[d] |
| A:T to G:C | 17 (56.7) | 11 (68.8) | 4 (17.4) | 10 (76.9) |
| A:T to T:A | 5 (16.7) | 2 (12.5) | 18 (78.3) | 2 (15.4) |
| A:T to C:G | 8 (26.7) | 3 (18.8) | 1 (4.3) | 1 (7.7) |
| Total | 30 (100%) | 16 (100%) | 23 (100%) | 13 (100%) |

[a]Site-specifically incorporated 1,$N^6$-ethenoadenine (5′-GCT(εA)GC-3′) in single strand M13DNA was replicated in *E.coli* cells (9).
[b]Site-specifically incorporated 4-amino-5-(imidazol-2-yl)imidazole (β) [5′-GCT(β)GC-3′] in single strand M13DNA was replicated in *E.coli* cells (9).
[c]The CAA treated gapped duplex M13DNA was replicated in UV-irradiated *E.coli* cells (13).
[d]Data contain all single, tandem and multiple base substitutions.

mutation fixation in *E.coli* and human cells, the contradicting results with M13 may be due to the difference in the sites of the adducts produced in DNA as the adducts are located in the single stranded region of the gap in the gapped duplex DNA (13).

The shuttle vector plasmid pMY189 designed to be applied to the fluorescent dye primer cycle sequencing by an automatic DNA sequencer, made the analysis of the nucleotide sequences of the mutant *supF* genes easier and faster than the conventional radioisotope labelling and autoradiography method. This method also made the analysis more accurate than the dye deoxy terminator cycle sequencing method using the automatic DNA sequencer we previously used (33).

In conclusion, we found that about half of the CAA-induced mutations were G:C to A:T transitions and that most of the remaining mutations were G:C to T:A transversions and A:T to G:C transitions in the shuttle vector plasmid pMY189 propagated in human cells. G:C pairs in 5′-AAGG-3′ or 5′-CCTT-3′ sequences are the major target of mutations, mainly, G:C to A:T transitions. This sequence specificity can be extrapolated to the estimation of contribution of VC to carcinogenesis in human beings.

## References


1. IARC (1987) *IARC Monographs*, International Agency for Research on Cancer, France, Supplement 7, pp. 373–376.
2. IARC (1987) *IARC Monographs*, International Agency for Research on Cancer, France, Supplement 6, pp. 566–569.
3. Laib,R.J., Gwinner,L.M. and Bolt,H.M. (1981) DNA alkylation by vinyl chloride metabolites: Etheno derivatives or 7-alkylation of guanine? *Chem.-Biol. Interactions*, **37**, 219–231.
4. Leonard,N.J. (1984) Etheno-substituted nucleotides and coenzymes: Fluorescence and biological activity. *CRC Crit. Rev. Biochem.*, **15**, 125–136.
5. Barbin,A. and Bartsch,H. (1986) Mutagenic and promutagenic properties of DNA adducts formed by vinyl chloride metabolites. In Singer,B. and Bartsch,H. (eds) *The Role of Cyclic Nucleic Acid Adducts in Carcinogenesis and Mutagenesis*. IARC Scientific Publication, Oxford University Press, London pp. 345–358.
6. Fedtke,N., Walker,V.E. and Swenberg,J.A. (1989) Determination of 7-(2′-oxoethyl) guanine and $N^2$,3-ethenoguanine in DNA hydrolysates by HPLC. *Arch. Toxicol. Suppl.*, **13**, 214–218.
7. Hall,J.A., Saffhill,R., Green,T. and Hathway,D.E. (1981) The induction of errors during *in vitro* DNA synthesis following chloroacetaldehyde-treatment of poly(dA-dT) and poly(dC-dG) templates. *Carcinogenesis*, **2**, 141–146.
8. Singer,B., Kusmierek,J.T., Folkman,W., Chavez,Z. and Dosanijh,M.K. (1991) Evidence for the mutagenic potential of the vinyl chloride induced adduct, $N^2$,3-etheno-deoxyguanosine, using a site-directed kinetic assay. *Carcinogenesis*, **12**, 745–747.
9. Basu,A.K., Wood,M.L., Niedernhofer,L.J., Ramos,L.A. and Essigmann,J.M. (1993) Mutagenic and genotoxic effects of three vinyl chloride-induced DNA lesions, 1,$N^6$-ethenoadenine, 3,$N^4$-ethenocytosine, and 4-amino-5-(imidazol-2-yl) imidazole. *Biochemistry*, **32**, 12 793–12 801.
10. Palejwala,V.A., Rzepka,R.W., Simha,D. and Humayun,M.Z. (1993) Quantitative multiplex sequence analysis of mutational hot spots. Frequency and specificity of mutations induced by a site-specific ethenocytosine in M13 viral DNA. *Biochemistry*, **32**, 4105–4111.
11. Cheng,K.C., Preston,B.D., Cahill,D.S., Dosanjh,M.K., Singer,B. and Loeb,L.A. (1991) The vinyl chloride DNA derivative $N^2$,3-ethenoguanine produces G→A transitions in *Escherichia coli*. *Proc. Natl Acad. Sci. USA*, **88**, 9974–9978.
12. Palejwala,V.A., Simha,D. and Humayun,M.Z. (1991) Mechanisms of mutagenesis by exocyclic DNA adducts. Transfection of M13 viral DNA bearing a site-specific adduct shows that ethenocytosine is a highly efficient *recA*-independent mutagenic noninstructional lesion. *Biochemistry*, **30**, 8736–8743.
13. Jacobsen,J.S. and Humayun,M.Z. (1990) Mechanisms of mutagenesis by the vinyl chloride metabolite chloroacetaldehyde. Effect of gene-targeted *in vitro* adduction of M13 DNA on DNA template activity *in vivo* and *in vitro*. *Biochemistry*, **29**, 496–504.
14. Marion,M.J., Froment,O. and Trepo,C. (1991) Activation of Ki-*ras* gene by point mutation in human liver angiosarcoma associated with vinyl chloride exposure. *Mol. Carcinogenesis*, **4**, 450–454.
15. Barbin,A., Besson,F., Perrard,M.H., Bereziat,J.C., Kaldor,J., Michel,G. and Bretsch,H. (1985) Induction of specific base-pair substitutions in *E.coli trpA* mutants by chloroethylene oxide, a carcinogenic vinyl chloride metabolite. *Mutat. Res.*, **152**, 147–156.
16. Kraemer,K.H. and Seidman,M.M. (1989) Use of *supF*, an *Escherichia coli* tyrosine suppressor tRNA gene, as a mutagenic target in shuttle-vector plasmids. *Mutat. Res.*, **220**, 61–72.
17. Levy,D.D., Groopman,J.D., Lim,S.E., Seidman,M.M. and Kraemer,K.H. (1992) Sequence specificity of aflatoxin $B_1$-induced mutations in a plasmid replicated in xeroderma pigmentosum and DNA repair proficient human cells. *Cancer Res.*, **52**, 5668–5673.
18. Moriwaki,S., Yagi,T., Nishigori,C., Imamura,S. and Takebe,H. (1991) Analysis of *N*-methyl-*N*-nitrosourea-induced mutations in a shuttle vector plasmid propagated in mouse $O^6$-methylguanine-DNA methyltransferase-deficient cells in comparison with proficient cells. *Cancer Res.*, **51**, 6219–6223.
19. Akasaka,S., Takimoto,K. and Yamamoto,K. (1992) G,C → T,A and G,C → C,G transversions are the predominant spontaneous mutations in the *Escherichia coli supF* gene; an improved *lacZ(am) E.coli* host designed for assaying pZ189 *supF* mutational specificity. *Mol. Gen. Genet.*, **235**, 173–178.
20. Girardi,A.J., Jensen,F.C. and Koprowski,H. (1965) SV40-induced transformation of human diploid cells, crisis and recovery. *J. Cell. Comp. Physiol.*, **65**, 69–84.
21. Takebe,H., Nii,S., Ishii,M. and Utsumi,H. (1974) Comparative studies of host-cell reactivation, colony forming ability and excision repair after UV irradiation of xeroderma pigmentosum, normal human and some other mammalian cells. *Mutat. Res.*, **25**, 383–390.
22. Seidman,M.M., Dixon,K., Razzaque,A., Zagursky,R. and Berman,M.L. (1985) A shuttle vector plasmid for studying carcinogen-induced point mutations in mammalian cells. *Gene*, **38**, 233–237.
23. Brash,D.E., Seetharam,S., Kraemer,K.H., Seidman,M.M. and Bredberg,A. (1987) Photoproduct frequency is not the major determinant of UV base substitution hot spots or cold spots in human cells. *Proc. Natl Acad. Sci. USA*, **84**, 3782–3786.
24. Moraes,E.C., Keyse,S.M., Pidoux,M. and Tyrrell,R.M. (1989) The spectrum of mutations generated by passage of a hydrogen peroxide damaged shuttle vector plasmid through a mammalian host. *Nucleic Acids Res.*, **17**, 8301–8312.
25. Bigger,C.A.H., Flickinger,D.J., Strandberg,J., Pataki,J., Harvey,R.G. and Dipple,A. (1990) Mutational specificity of the *anti* 1,2-dihydrodiol 3,4-epoxide of 5-methylchrysene. *Carcinogenesis*, **11**, 2263–2265.
26. Moraes,E.C., Keyse,S.M. and Tyrrell,R.M. (1990) Mutagenesis by hydrogen peroxide treatment of mammalian cells, a molecular analysis. *Carcinogenesis*, **11**, 283–293.
27. Wang,P., Bennett,R.A.O. and Povirk,L.F. (1990) Melphalan-induced mutagenesis in an SV40-based shuttle vector, Predominance of A,T →

T,A transversions. *Cancer Res.*, **50**, 7527–7531.
28. Akman,S.A., Forrest,G.P., Doroshow,J.H. and Dizdaroglu,M. (1991) Mutation of potassium permanganate- and hydrogen peroxide-treated plasmid pZ189 replicating in CV-1 monkey kidney cells. *Mutat. Res.*, **261**, 123–130.
29. Bigger,C.A.H., Flickinger,D.J., John,J.S., Harvey,R.G. and Dipple,A. (1991) Preferential mutagenesis at G,C base pairs by the anti 3,4-dihydrodiol 1,2-epoxide of the 7-methylbenz[*a*]anthracene. *Mol. Carcinogenesis*, **4**, 176–179.
30. Bubley,G.J., Ashburner,B.P. and Teicher,B.A. (1991) Spectrum of *cis*-diamminedichloroplatinum(II)-induced mutations in a shuttle vector propagated in human cells. *Mol. Carcinogenesis*, **4**, 397–406.
31. Seetharam,S., Kraemer,K.H., Waters,H.L. and Seidman,M.M. (1991) Ultraviolet mutational spectrum in a shuttle vector propagated in xeroderma pigmentosum lymphoblastoid cells and fibroblasts. *Mutat. Res.*, **254**, 97–105.
32. Seetharam,S. and Seidman,M.M. (1991) Modulation of an ultraviolet mutational hotspot in a shuttle vector in xeroderma cells. *Nucleic Acids Res.*, **19**, 1601–1604.
33. Yagi,T., Tatsumi-Miyajima,J., Sato,M., Kraemer,K.H. and Takebe,H. (1991) Analysis of point mutations in an ultraviolet-irradiated shuttle vector plasmid propagated in cells from Japanese xeroderma pigmentosum patients in complementation groups A and F. *Cancer Res.*, **51**, 3177–3182.
34. Bigger,C.A.H., John,J.S., Yagi,H., Jerina,D.M. and Dipple,A. (1992) Mutagenic specificities of four stereoisomeric benzo[c]phenanthrene dihydrodiol epoxides. *Proc. Natl Acad. Sci. USA*, **89**, 368–372.
35. Yagi,T., Sato,M., Tatsumi-Miyajima,J. and Takebe,H. (1992) UV-induced base substitution mutations in a shuttle vector plasmid propagated in group C xeroderma pigmentosum cells. *Mutat. Res.*, **273**, 213–220.
36. Madzak,C., Armier,J., Stary,A., Daya-Grosjean,L. and Sarasin,A. (1993) UV-induced mutations in a shuttle vector replicated in repair deficient trichothiodystrophy cells differ with those in genetically-related cancer prone xeroderma pigmentosum. *Carcinogenesis*, **14**, 1255–1260.
37. Routledge,M.N., Wink,D.A., Keefer,L.K. and Dipple,A. (1993) Mutations induced by saturated aqueous nitric oxide in the pSP189 *supF* gene in human Ad293 and *E.coli* MBM7070 cells. *Carcinogenesis*, **14**, 1251–1254.
38. Akasaka,S. and Yamamoto,K. (1994) Hydrogen peroxide induces G:C to C:G transversions in the *supF* gene of *Escherichia coli*. *Mol. Gen. Genet.*, **243**, 500–505.
39. Yagi,T., Sato,M., Nishigori,C. and Takebe,H. (1994) Similarity in the molecular profile of mutations induced by UV light in shuttle vector plasmids propagated in mouse and human cells. *Mutagenesis*, **9**, 73–77.
40. Dosanjh,M.K., Chenna,A., Kim,E., Fraenkel-Conrat,H., Samson,L. and Singer,B. (1994) All four known cyclic adducts formed in DNA by the vinyl chloride metabolite chloroacetaldehyde are released by a human DNA glycosylase. *Proc. Natl Acad. Sci. USA*, **91**, 1024–1028.
41. Dosanijh,M.K., Roy,R., Mitra,S. and Singer,B. (1994) 1,$N^6$-Ethenoadenine is preferred over 3-methyladenine as substrate by a cloned human *N*-methylpurine-DNA glycosylase (3-methyladenine-DNA glycosylase). *Biochemistry*, **33**, 1624–1628.
42. Wood,R.D., Scopek,T.R. and Hutchinson,F. (1984) Changes in DNA base sequence induced by targeted mutagenesis of lambda phage by ultraviolet light. *J. Mol. Biol.*, **173**, 273–291.

*Received on February 9, 1995; revised on June 26, 1995; accepted on July 18, 1995*

Nucleic Acids Research, 2002, Vol. 30, No. 6 1387–1393

# Transcriptional regulation of the mouse steroid 5α-reductase type II gene by progesterone in brain

**Daisuke Matsui[1], Matomo Sakari[1], Takashi Sato[1,2], Akiko Murayama[1], Ichiro Takada[1,2], Misun Kim[1], Ken-ichi Takeyama[1,2] and Shigeaki Kato[1]***

[1]Institute of Molecular and Cellular Biosciences, University of Tokyo, Tokyo 113-0032, Japan and [2]Core Research for Evolutional Science and Technology, Japan Science and Technology Corporation, Saitama 332-0012, Japan

Received October 24, 2001; Revised and Accepted January 22, 2002

DDBJ/EMBL/GenBank accession nos AB049455 and AB049456

## ABSTRACT

**The steroid 5α-reductase (5α-R) plays an important physiological role in the conversion of steroid hormones such as androgen and progesterone to their 5α-reduced derivatives. 5α-R type II (5α-R2), one of two 5α-R isoforms, is thought to be a key enzyme in the generation of neuroactive steroids in the brain, particularly allopregnanolone (AP), via the production of its precursor dihydroprogesterone from progesterone. In the present study, we investigated possible regulatory mechanisms of 5α-R2 gene expression by steroid hormones in the female mouse brain. We first cloned mouse 5α-R2 (m5α-R2) cDNA by degenerate PCR, and found that progesterone induced 5α-R2 gene expression to levels detectable by *in situ* hybridization in female mouse brains. Functional analysis of the m5α-R2 gene promoter by a transient expression assay with human progesterone receptor (PR) and androgen receptor (AR) expression vectors identified a progesterone and androgen regulatory element (m5α-R2 PRE/ARE). Results of an electrophoretic mobility shift assay revealed that both PR and AR homodimers bound directly to m5α-R2 PRE/ARE sequence. These findings suggest that the gene expression of m5α-R2 is transcriptionally regulated by progesterone in female brains.**

## INTRODUCTION

The steroid 5α-reductase (5α-R) is a key enzyme in the conversion of several Δ4-3keto steroids such as testosterone, progesterone, aldosterone and corticosterone, into their respective 5α-reduced derivatives (1–3). Two isoforms of 5α-R have been identified. While these isoforms catalyze the same reaction, they possess different biochemical and pharmacological properties, and display distinct expression patterns in tissues (4–7). Type I (5α-R1) is widely distributed throughout the body, and is most abundant in the liver where it catabolizes steroids. Type II (5α-R2) is primarily expressed in target tissues for androgens, such as the prostate and seminal vesicles, and is responsible for converting testosterone into dihydrotestosterone (DHT), a potent natural androgen. Impaired 5α-R2 activity caused by mutations in the human 5α-R2 gene results in insufficient DHT production, leading to male pseudohermaphroditism (5,8). Recently, it was found that 5α-R2 was expressed in male rat brains at detectable levels after testosterone was given. This raised the possibility that the testosterone-induced up-regulation of 5α-R2 gene expression and resultant enhanced production of DHT was important for mediating the male sexual behavior and aggression that occurred during a very critical period (9). In contrast, the physiological role of 5α-R2 in the female brain remains largely unknown.

5α-R2 is also known to metabolize progesterone into dihydroprogesterone (DHP), and DHP is further converted into allopregnanolene (AP) by 3α-hydroxysteroid dehydrogenase (3α-HSD) (10,11). AP is thought to exert anti-convulsant and anxiolytic-like actions (12,13) by binding to allosteric sites on neurotransmitter-gated ion channels, such as the γ-amino butyric acid type A ($GABA_A$) receptor (14–16). When brain progesterone and AP levels are increased during pregnancy or transient stress, expression of genes for $GABA_A$ receptor inhibitory subunits α4 (17–20) were shown to be down-regulated, possibly resulting in the potentiation of AP action through enhanced $GABA_A$ receptor function. Nonetheless, there is little information concerning the effects of progesterone on 5α-R2 gene expression in the female brain.

Androgens and progesterone are believed to mediate their effects through the transcriptional control of specific sets of target genes via nuclear receptors (21–23). Androgen receptor (AR) and progesterone receptor (PR) are members of the nuclear receptor superfamily, and act as hormone-inducible transcription factors that bind specific DNA elements as homodimers (24–28). The DNA elements that bind AR and PR share the common sequence 5′-AGAACANNNTGTTCT-3′, known as the consensus progesterone/androgen response element (PRE/ARE) (29). As both hormone receptors recognize the same sequence, it is likely that the same genes are regulated when either AR or PR are present in a given tissue or cell (30–33). Therefore, the fact that the transcriptional control of 5α-R2 is regulated by the DHT–AR system in the male brain raises the

*To whom correspondence should be addressed at: Institute of Molecular and Cellular Biosciences, University of Tokyo, Yayoi 1-1-1, Bunkyo-ku, Tokyo 113-0022, Japan. Tel: +81 3 5841 8478; Fax: +81 3 5841 8477; Email: uskato@mail.ecc.u-tokyo.ac.jp

possibility that progesterone may act as a positive regulator for 5α-R2 gene expression in the female brain.

To test this hypothesis, the present study was undertaken to examine 5α-R2 gene expression in female mice. First, the cDNA of mouse 5α-R2 (m5α-R2) was amplified by degenerate PCR and cloned. The 5α-R2 gene expression was induced by the treatment of either progesterone or androgen in female mouse brains. *In situ* analyses of female brains detected the 5α-R2 transcript in the hippocampus of the mice treated with progesterone. Furthermore, the putative PRE/ARE was identified in the m5α-R2 gene promoter. Thus, our results suggested that the progesterone-induced expression of 5α-R2 promoted AP production in the female brain.

## MATERIALS AND METHODS

### RNA isolation and molecular cloning of 5α-R2 cDNA in the mouse kidney

Total RNA was isolated from kidneys of 10-week-old female mice (ICR CD1; Charles River Laboratories, Inc.) using isogen solution (Nippongene) and reverse transcribed using an oligo(dT)$_{18}$ primer and SuperScript II reverse transcriptase (Life Technologies, Inc.). Degenerate PCR was then performed using specific primers based on homologous regions of rat and human 5α-R2 sequences (1,4,8): 5′-ATGCAGATTGTCTGCCAKCAG-3′ (nucleotides 1–21) and 5′-TTAAAAGATGAATGGAAT-3′ (nucleotides 745–765). PCR products of the expected size (765 bp) were subcloned into the pcDNA3 expression vector under control of the cytomegalovirus promoter (Invitrogen), and subjected to sequence analysis using a Prism 377 DNA (Applied Biosystems).

### Plasmid construction

cDNA encoding m5α-R2 and the mutant G34R (34) was subcloned into the pcDNA3 (Invitrogen) expression vector. A series of deletion mutants of the m5α-R2 gene promoter, consensus PRE/ARE (5′-AGAACATCCTGTTCT-3′) (×2) with the thymidine kinase (tk) short promoter, and m5α-R2 PRE/ARE ×2 with the tk short promoter were subcloned into the pGL3 reporter plasmid (Invitrogen). The 5′-flanking region of the m5α-R2 gene was isolated by the inverse PCR. Primers recognizing the predicted start of exon 1 (5′-CCAAAGCACA-GGATCAGGGT-3′), and predicted end of exon 1 5′-TTGGAC-CTCCGGGGAATGTG-3′) were used to amplify product from circularized genomic DNA.

### Converting activity of 5α-R2

5α-R2 activity was assayed using the nuclear receptor-mediated transactivation method (35), COS-1 cells were maintained in DMEM without phenol red and supplemented with 5% FBS stripped with dextran-coated charcoal. Cells cultured with precursors were transiently transfected with 50 and 5 ng expression vectors for nuclear receptors and m5α-R2, respectively, and 0.5 μg reporter plasmid (Firefly luciferase) using the Lipofectin reagent (Gibco BRL). Bluescribe M13$^+$ (Stratagene) was used as a carrier to adjust the total amount of DNA to 1.5 μg for transfection and 1 nM steroid hormone used as a positive control. Transfection efficiency was normalized according to Renilla luciferase activity (derived from pRL-CMV) as an internal control. The m5α-R2 enzyme activity was assayed also by *in vitro* converting method (36) with the cell extract (10 mM Tris–HCl pH 5.0, 150 mM NaCl, 1 mM EDTA, 10% glycerol) of COS-1 cells transfected with the m5α-R2, rat 5α-R2 or mutant G34R expression plasmids. The cell extracts (30 μg protein) were incubated in 0.1 M Tris–HCl buffer pH 5.0 containing either 5 μM [$^{14}$C]teststerone or progesterone (NEN™ Life Science Product) and 5 mM NADPH (Sigma) for 1 h at 37°C. The labeled steroids were extracted into methylene chroride, resuspended in chloroform–methanol (3:1, v/v) and developed by chloroform–ethylacetate (2:1, v/v) onto Silica Gel 60 $F_{254}$ TLC plates (Merck) with the detection of converted steroids by autoradiography.

### Animals and experimental protocols

Ten-week-old female mice, weighing ~20 g, were fed a standard rodent chow with free access to food and tap water. Four hours after subcutaneous injection of progesterone (500 μg/mouse) or testosterone (500 μg/mouse), the mice were sacrificed according to principles and procedures outlined in the NIH Guide for the Care and Use of Laboratory Animals.

### *In situ* hybridization

Brain tissues were fixed in 4% paraformaldehyde, and dehydrated with increasing concentrations of ethanol prior to paraffin embedding. Antisense and sense riboprobes were generated from nucleotides 1–765 of m5α-R2 cDNA in pcDNA3 using the DIG RNA labeling kit (Boehringer Mannhein). Paraffin-embedded tissue sections of adult mouse brain were placed on microscope slides, hybridized to riboprobes, and incubated with horseradish peroxidase-conjugated anti-DIG antibody (Boehringer Mannhein) using the ISHR starting kit (Nippongene). For *in situ* hybridization signal amplification, the slides were incubated with biotinyl tyramide and horseradish peroxidase-conjugated streptavidin using the TSA™-INDIRECT kit (NEN™ Life Science Products) and stained with diaminobenzidine.

### Semi-quantitative RT–PCR

Aliquots of total RNA (3 μg) extracted from mouse brains were reverse-transcribed using the SuperScript pre-amplification system (Gibco BRL) according to the manufacturer's instructions. PCR was performed in a 25 μl reaction volume containing 1 μl 1/20 reverse transcription mix solution, 0.4 μM primers, 0.25 mM dNTPs and 0.125 U AmpliTaq Gold DNA polymerase (Perkin-Elmer). After 5 min pre-incubation at 96°C, amplification of mouse 5α-R2, histidine decarboxylase (HDC) (37) or β-actin cDNA was performed for 35, 35 or 25 cycles, respectively. Cycles consisted of 1 min denaturation at 96°C, 1 min annealing at 56°C and 1 min extension at 72°C. Primers sets used were as follows: 5′-TTGGACCTCCGGGGAATGTG-3′ and 5′-GGCTG-GAACAGACCAAGTGG-3′ for m5α-R2, 5′-CATCAAGCAGC-CAGGAGCCAGTCTG-3′ and 5′-GCACGGTAGCTGGCGA-GCACACTG-3′ for mouse HDC, 5′-TGGAATCCTGTGGCATC-CATGAAACT-3′ and 5′-TAAAACGCAGCTCAGTAACTGT-CCG-3′ for mouse β-actin.

### Primer extension analysis

Poly(A)$^+$ RNA was isolated from total RNA by oligo(dT) affinity chromatography and 1 μg mixed with 2 pmol 5′-$^{32}$P-labeled primer corresponding to nucleotides 55 bp downstream from the translational start site (5′-TGGCCAATGTGGCGCTACCT-3′).

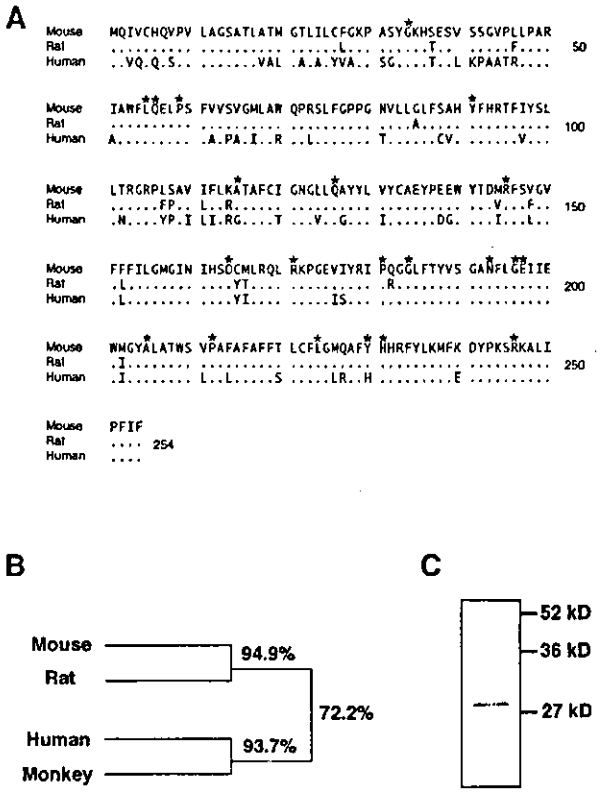


**Figure 1.** Molecular cloning of m5α-R2 cDNA. (**A**) Predicted amino acid sequence comparison of 5α-R2 protein between mouse and other species. Asterisks indicate the point mutation sites found in human 5α-R2 deficiency disease (34). (**B**) Homology between the mouse, rat, human and monkey 5α-R2 proteins (2). (**C**) *In vitro*-translated m5α-R2 protein. m5α-R2 protein *in vitro* translated in the presence of $^{35}$S-labeled methionine using the reticulocyte lysate system (Promega) was analyzed by 10% SDS–PAGE.

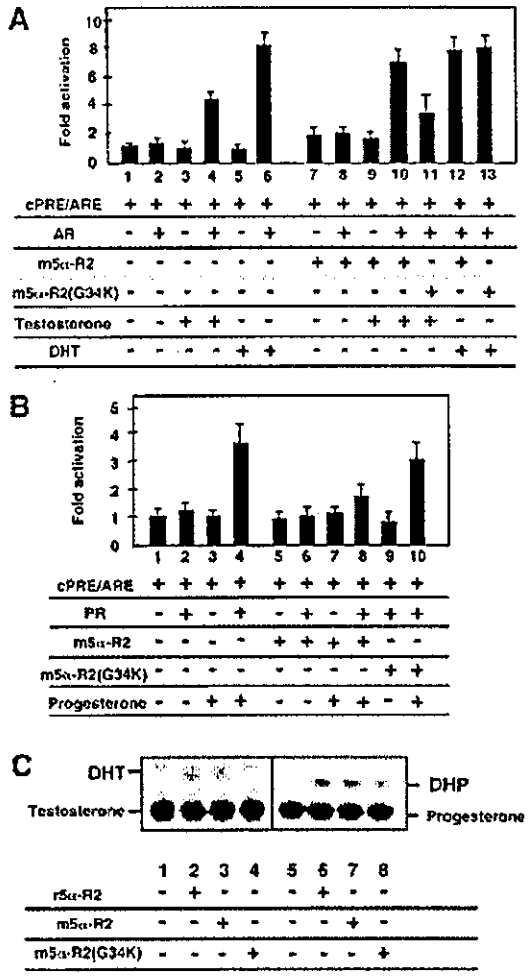


**Figure 2.** Enzyme activity of m5α-R2 transiently transfected in COS-1 cells. Conversion of testosterone, serving as an AR ligand, into DHT, a potent ligand for AR (**A**); and progesterone, serving as a PR ligand, into the inactive ligand DHP (**B**) by m5α-R2. COS-1 cells were co-transfected with the luciferase reporter plasmid containing two copies of consensus PRE/ARE (cPRE/ARE), and the expression plasmids containing AR, PR, m5α-R2 or m5α-R2 mutant (G34R), with or without the indicated ligands. Human 5α-R2 mutant G34R results in reduced enzyme activity (34). Fold luciferase activities corresponding to means ± SEM for three independent experiments are shown. *In vitro* converting method (**C**) was described in the Materials and Methods (36). The conversions of testosterone into DHT and progesterone into DHP by 5α-R2 are shown in lanes 1–4 or 5–8, respectively. r5α-R2, rat 5α-R2 (4).

Reactions were denatured by heating at 60°C for 60 min, then annealed at room temperature for 90 min. Primer extension proceeded at 37°C for 60 min with 15 U/μl of SuperScript II reverse transcriptase (Gibco BRL), 1× first strand buffer, 75 mM KCl, 3 mM $MgCl_2$, 10 mM DTT and 0.4 mM dNTPs. After ethanol precipitation, products were analyzed on 8% acrylamide–7 M urea sequence gels. The subcloned 5′-flanking region was sequenced using the same primer using the Sequencing PRO DNA Sequencing Kit (Toyobo) and electrophoresed on the same gel (38).

### Electrophoretic mobility shift assay (EMSA)

Nuclear extracts were prepared from COS-1 cells transfected with the expression plasmids. Reaction mixtures in the absence or presence of cold consensus PRE/ARE were incubated for 30 min on ice in binding buffer (5 mM Tris–HCl pH 8.0, 40 mM KCl, 6% glycerol, 1 mM DTT, 0.05% Nonidet P-40), and 2 μg of poly(deoxyinosinic-deoxycytidylic) acid in a final volume of 20 μl. Double-stranded consensus PRE/ARE (5′-ggggtac-cAGAACATCCTGTTCTggtacccc-3′) and m5α-R2 PRE/ARE (5′-catgtgaGGGACAAACTTTTCTccaaggct-3′) DNA fragments were end-labeled using [γ-$^{32}$P]ATP and T4 polynucleotide kinase and used as probes. PRE/ARE DNA fragments were added to the mixtures, and further incubated for 20 min at room temperature. Entire reaction mixtures (20 μl) were then loaded onto 4.5% polyacrylamide gels in 0.25× TAE buffer and electrophoresed at 4°C. The gels were dried on filter paper and exposed to X-ray film (39,40).

## RESULTS

### cDNA cloning of mouse 5α-reductase type II (5α-R2)

m5α-R2 cDNA was isolated by PCR amplification using degenerate primers based on homologous sequences between human and rat 5α-R2 cDNAs. The isolated cDNA (765 bp)

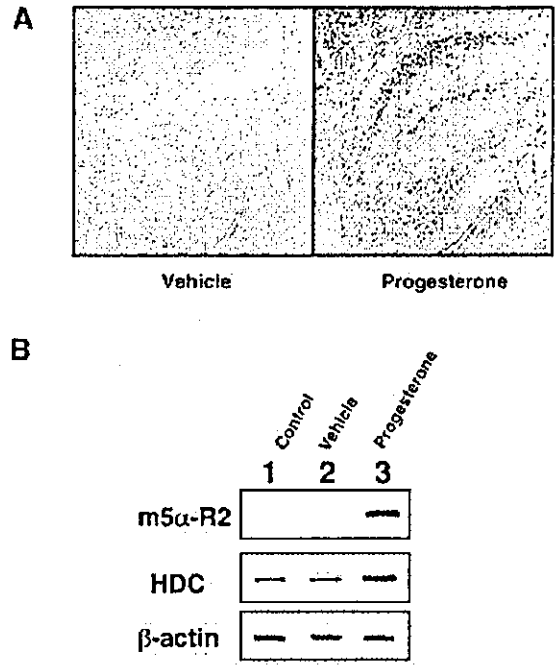


Figure 3. Induction of m5α-R2 gene expression in adult female mice brains by the administration of progesterone. m5α-R2 gene expression was detected by *in situ* hybridization (A), and semi-quantitative RT–PCR (B) in the brains of female adult mice to which 500 μg of progesterone had been administrated 4 h previously. (A) m5α-R2 gene expression induced by progesterone was detected in the hippocampus. (B) Bands were obtained by semi-quantitative RT–PCR on total RNA extracted from individual mouse brains with or without the administration of progesterone. HDC was used as a positive control for progesterone administration (37). m5α-R2 gene expression was induced by progesterone in the female adult brain.

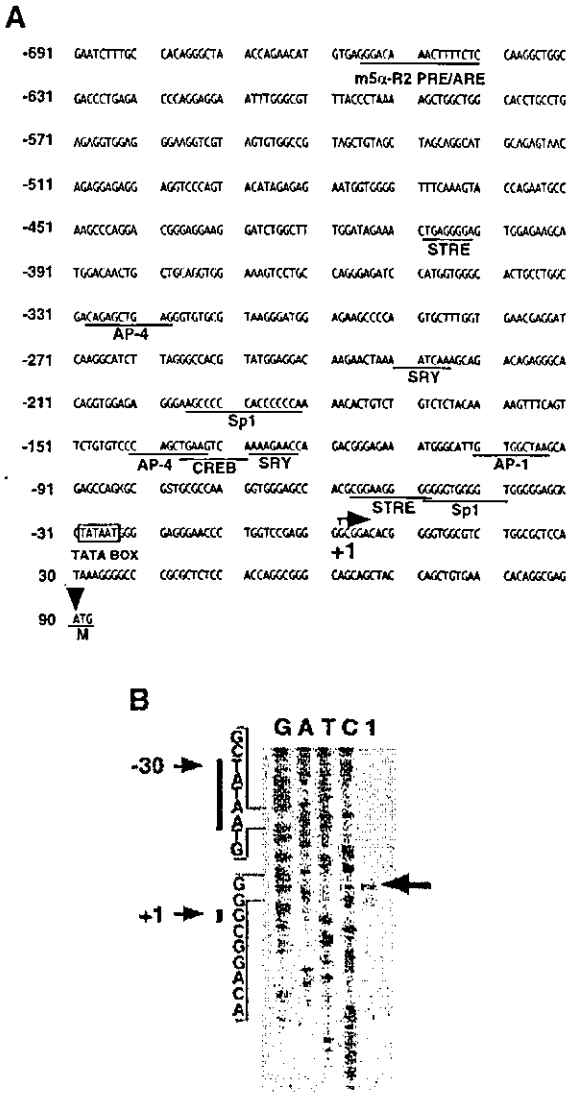


Figure 4. Promoter analysis of the m5α-R2 gene. (A) Nucleotide sequence of the 5′-flanking region of m5α-R2. Transcription start site is designated as +1, and putative *cis* regulatory elements are underlined. Translational start codon is indicated by closed triangle (+90). STRE, stress-response element; AP-4, activator protein 4; SRY, sex-determining region Y gene product; Sp1, stimulating protein 1; CREB, cAMP-responsive element binding protein; AP-1, activator protein 1; M, initiation codon. (B) Identification of the transcription start site of the m5α-R2 gene. Primer extension analysis of mouse kidney 5α-R2 mRNA was performed using 1 μg poly(A)$^+$ RNA (lane 1) using a labeled primer. Primer extension products were co-electrophoresed with sequencing reaction products using the same primer to determine the precise start site. The major transcription start site (+1) is indicated by an arrow on the right, and the position of the TATA box (–30) is indicated by an arrow on the left.

contained an ORF that encoded a putative 254 amino acid protein that showed high similarity to rat (94.9%) and human (75.7%) 5α-R2 sequences (Fig. 1A and B) (1). Amino acids critical for enzymatic function assumed from human genetic diseases were mostly identical to those mouse and rat sequences (indicated by asterisks, Fig. 1A) (5,34). The cloned m5α-R2 cDNA was *in vitro* translated resulting in a 29 kDa protein (Fig. 1C), in agreement with the predicted molecular size.

We then tested the enzymatic activity of the recombinant m5α-R2 using a nuclear receptor-mediated transactivation system (35). This system is based on the principle that the transactivation function of a nuclear receptor is initiated only by its endogenous ligand, and not by ligand precursors or metabolites (16). In the present study, the ability of m5α-R2 to metabolize androgen and progesterone was assessed with respect to the ligand-induced transactivation functions of AR and PR. While AR transactivation function was clearly induced by DHT, only a slight induction by testosterone was seen (Fig. 2A). The expression of m5α-R2 led to a 2-fold increase in testosterone-induced AR transactivation function (Fig. 2A, compare lanes 4 and 10). However, a putative inactivation mutant of m5α-R2 (G34R) failed to potentiate testosterone-induced AR transactivation function (34). Thus, our results suggested that the enzymatic conversion of testosterone into DHT was mediated by m5α-R2. Unlike the enhanced transactivation of testosterone-bound AR by m5α-R2, the progesterone-induced transactivation function of PR was reduced by the presence of m5α-R2 (Fig. 2B, compare lanes 4 and 8). This was due to the metabolic inactivation of progesterone into DHP, as mutant 5α-R2 (G34R) did not exhibit this effect. Moreover, we performed the *in vitro* converting assay (36) to confirm the 5α-R2 enzyme activity (Fig. 2C). The conversions of

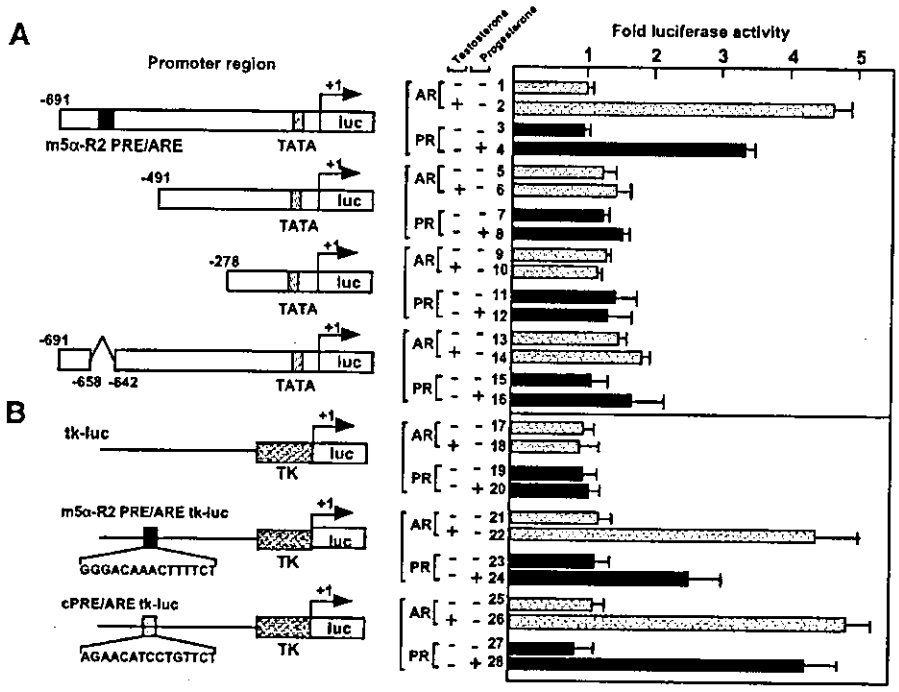


**Figure 5.** Identification of the positive regulatory region for progesterone or testosterone in the m5α-R2 gene promoter. COS-1 cells were transiently co-transfected with the luciferase reporter plasmid containing the indicated promoter regions of the m5α-R2 gene (A), putative m5α-R2 PRE/ARE in the promoter region, or cPRE/ARE (B), and AR or PR expression plasmids with 10 nM testosterone or progesterone, respectively. Fold increases in luciferase activity are based on each of the activities without ligand. Fold luciferase activities corresponding to means ± SEM for three independent experiments are shown.

testosterone into DHT and progesterone into DHP by 5α-R2 were detected with equal efficiency by the rat 5α-R2 enzyme (Fig. 2C, compare lanes 2 and 3, or lanes 6 and 7). Thus, the cloned m5α-R2 appeared to possess the expected activities in steroid metabolism.

### Progesterone-induced 5α-R2 gene expression in the hippocampus of female brains

As m5α-R2 is thought to metabolize steroids into neurosteroids in the brain, the expression of 5α-R2 was examined in male and female mouse brains. No expression was detected in female brains by *in situ* hybridization. However, 4 h after the administration of progesterone (500 μg per mouse), clear m5α-R2 mRNA expression was detected in the hippocampus (Fig. 3A). RT–PCR (Fig. 3B) and northern blotting analyses confirmed the induction of the m5α-R2 gene in female brains by progesterone, while androgen induced the m5α-R2 gene in the male brain (data not shown) as expected from previous reports (9).

### Isolation of the 5′-flanking region of the m5α-R2 gene and identification of the transcription initiation site

To address whether m5α-R2 gene induction in female brains by progesterone involved transcriptional or post-transcriptional mechanisms, we directly assessed the promoter function of the m5α-R2 gene. We first isolated the 5′-flanking region of the 5α-R2 by inverse-PCR using primers that corresponded to the exon 1 sequence, and a genomic fragment 780 bp upstream of the putative translation start site (ATG codon) was cloned (Fig. 4A) (41). Using this cloned genomic fragment, the transcription start site was determined by the primer extension method (38). Results indicated that the start site was located 89 bp upstream of the ORF, with a TATA box 30 bp upstream (Fig. 4A and B). A sequence closely related to the consensus PRE/ARE sequence (designated as m5α-R2 PRE/ARE hereafter) was present 657 bp upstream of the transcription start site, indicating possible regulation by progesterone and androgen via this element.

### Identification of a progesterone/audrogen response element (PRE/ARE) in the m5α-R2 gene promoter

We then tested the function of the PRE/ARE-like sequence of m5α-R2 using a transient expression assay with expression vectors for PR and AR in COS-1 cells, and luciferase reporter plasmids bearing a series of the deletion mutants of the m5α-R2 gene promoter (Fig. 4A). Promoters with the intact m5α-R2 PRE/ARE conferred both androgen- and progesterone-specific responses in the presence of cognate receptor. However, deletion of m5α-R2 PRE/ARE caused complete loss of responsiveness to progesterone and androgen without reduction of basal m5α-R2 gene promoter activity (Fig. 5A). Like consensus PRE/ARE, m5α-R2 PRE/ARE conferred responsiveness to both hormones even when driven by the basal thymidine kinase (tk) promoter (Fig. 5B).

We then examined whether AR or PR homodimers directly bound to the identified m5α-R2 PRE/ARE. An EMSA was performed using the consensus PRE/ARE prepared for the transient expression assay (Fig. 5B) as a positive control. As shown in Figure 6, both AR and PR effectively bound both consensus and m5α-R2 PRE/ARE sequences (Fig. 6, lanes 2 and 5; 9 and 12). Moreover, in the presence of excess cold

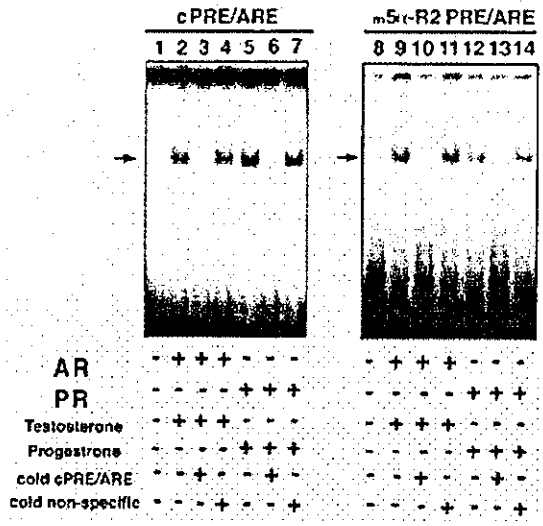


Figure 6. m5α-R2 PRE/ARE binding by AR and PR. EMSA was performed using [γ-$^{32}$P]ATP-labeled consensus PRE/ARE (lanes 1–7) or m5α-R2 PRE/ARE (lanes 8–14). COS-1 cells were transfected with AR (lanes 2, 3, 4, 9, 10 and 11) or PR (lanes 5, 6, 7, 12, 13 and 14) expression plasmid, and nuclear extracts were assayed. After incubation at room temperature with the indicated labeled probes, the nuclear extracts were electrophoresed on 4.5% polyacrylamide gels under non-denaturing conditions. Arrows indicate bound AR or PR. Cold consensus PRE/ARE and cold non-specific indicate non-labeled probes used for competition assay (lanes 3, 6, 10 and 13) and negative control (lanes 4, 7, 11 and 14), respectively.

consensus PRE/ARE DNA, AR and PR binding was abolished (Fig. 6, lanes 3 and 6; 10 and 13). Thus, taken together, our results suggested that both hormone-bound steroid receptors controlled m5α-R2 gene transcription through m5α-R2 PRE/ARE.

## DISCUSSION

To clarify the physiological roles of 5α-R2 in the activity of hormonal and neuroactive steroids in the brain, we studied the possible regulation of m5α-R2 gene expression by one of its enzymatic substrates, progesterone. We first cloned the m5α-R2 cDNA by degenerate PCR, and found that recombinant m5α-R2 protein expressed in cultured cells metabolized progesterone and androgen as shown using a nuclear receptor-mediated assay (35). Using the cDNA clone as an *in situ* hybridization probe, we found that m5α-R2 gene expression was undetectable in the female brain, but was induced up to detectable levels in the hippocampus of female mice by progesterone. A progesterone regulatory element was identified as a highly related sequence to the consensus PRE/ARE sequence in the m5α-R2 promoter, and this element, m5α-R2 PRE/ARE, was found to confer responsiveness to both progesterone and androgen, similar to consensus PRE/ARE. Thus, transcriptional control of m5α-R2 gene expression by progesterone and androgen appeared to be mediated through m5α-R2 PRE/ARE.

Neuroactive steroids, like AP, are thought to exert behavioral effects such as convulsant and anxiolytic-like actions through the modulation of neurotransmitter-gated iron channel functions through direct binding of their allosteric sites (43). The effects of neuroactive steroids, especially progesterone derivatives, appear to be more prominent in females with premenstrual syndrome (PMS) (18) or under transient stress (44). Lowered serum progesterone levels may lead to PMS due to insufficient production of neuroactive steroids in the female brain. In contrast, enhanced production of progesterone during pregnancy is thought to promote the production of neuroactive steroids. As 5α-R2 converts progesterone into DHP, the precursor of AP, 5α-R2 enzymatic activity in the female brain is likely to be physiologically important for the action of neuroactive steroids. The significant induction of m5α-R2 by progesterone in female brains was detected only in the hippocampus. Therefore, the physiological role of 5α-R2 in the hippocampus needs to be verified by specific disruption of the 5α-R2 gene in the hippocampus in further animal experiments.

The promoter of the m5α-R2 gene harbored several potential binding sites for distinct classes of transcription regulatory factors in addition to PR/AR. Among these, the presence of two SRY binding sites raises the possibility that m5α-R2 gene expression is induced to convert testosterone into the more active form DHT during embryogenesis to develop male reproductive organs, when SRY plays a critical role in sex determination (45). Moreover, due to the identification of a PRE/ARE in the m5α-R2 gene promoter presented in this study, it is possible that positive feedback regulation of m5α-R2 gene expression by androgen occurs during male reproductive organ development and may occur in adult males to maintain reproductive organ function. Indeed, genetic mutations in 5α-R2 that impair its enzymatic activity are known to cause the hereditary disease male pseudohermaphroditism (5,8), clearly indicating the indispensability of this enzyme in males. However, the physiological role of 5α-R2 in females remains to be examined in more detail during embryogenesis and in adulthood.

## ACKNOWLEDGEMENTS

We thank S. Kitanaka, T. Yoshizawa, T. Kawano, Y. Yamamoto, Y. Kodera, M. Suzawa and T. Matsumoto for helpful technical advice, and J. Yanagisawa, S. Sasagawa, T. Watanabe and T. Hashimoto for valuable discussions and technical assistance.

## REFERENCES

1. Andersson,S., Berman,D.M., Jenkins,E.P. and Russell,D.W. (1991) Deletion of steroid 5 alpha-reductase 2 gene in male pseudohermaphroditism. *Nature*, **354**, 159–161.
2. Levy,M.A., Brandt,M., Sheedy,K.M., Holt,D.A., Heaslip,J.I., Trill,J.J., Ryan,P.J., Morris,R.A., Garrison,L.M. and Bergsma,D.J. (1995) Cloning, expression and functional characterization of type 1 and type 2 steroid 5 alpha-reductases from Cynomolgus monkey: comparisons with human and rat isoenzymes. *J. Steroid Biochem. Mol. Biol.*, **52**, 307–319.
3. Poletti,A., Coscarella,A., Negri,C.P., Colciago,A., Celotti,F. and Martini,L. (1998) 5 Alpha-reductase isozymes in the central nervous system. *Steroids*, **63**, 246–251.
4. Normington,K. and Russell,D.W. (1992) Tissue distribution and kinetic characteristics of rat steroid 5 alpha-reductase isozymes. Evidence for distinct physiological functions. *J. Biol. Chem.*, **267**, 19548–19554.
5. Wilson,J.D., Griffin,J.E. and Russell,D.W. (1993) Steroid 5 alpha-reductase 2 deficiency. *Endocrine Rev.*, **14**, 577–593.
6. Russell,D.W. and Wilson,J.D. (1994) Steroid 5 alpha-reductase: two genes/two enzymes. *Annu. Rev. Biochem.*, **63**, 25–61.
7. Mahendroo,M.S., Cala,K.M. and Russell,D.W. (1996) 5 Alpha-reduced androgens play a key role in murine parturition. *Mol. Endocrinol.*, **10**, 380–392.

8. Andersson,S. and Russell,D.W. (1990) Structural and biochemical properties of cloned and expressed human and rat steroid 5 alpha-reductases. *Proc. Natl Acad. Sci. USA*, **87**, 3640–3644.
9. Poletti,A., Negri,C.P., Rabuffetti,M., Colciago,A., Celotti,F. and Martini,L. (1998) Transient expression of the 5alpha-reductase type 2 isozyme in the rat brain in late fetal and early postnatal life. *Endocrinology*, **139**, 2171–2178.
10. Celotti,F., Negri,C.P. and Poletti,A. (1997) Steroid metabolism in the mammalian brain: 5alpha-reduction and aromatization. *Brain Res. Bullet.*, **44**, 365–375.
11. Guidotti,A. and Costa,E. (1998) Can the antidysphoric and anxiolytic profiles of selective serotonin reuptake inhibitors be related to their ability to increase brain 3 alpha, 5 alpha-tetrahydroprogesterone (allopregnanolone) availability? *Biol. Psychiatry*, **44**, 865–873.
12. Mendelson,W.B., Martin,J.V., Perlis,M., Wagner,R., Majewska,M.D. and Paul,S.M. (1987) Sleep induction by an adrenal steroid in the rat. *Psychopharmacology (Berl.)*, **93**, 226–229.
13. Paul,S.M. and Purdy,R.H. (1992) Neuroactive steroids. *FASEB J.*, **6**, 2311–2322.
14. Majewska,M.D., Harrison,N.L., Schwartz,R.D., Barker,J.L. and Paul,S.M. (1986) Steroid hormone metabolites are barbiturate-like modulators of the GABA receptor. *Science*, **232**, 1004–1007.
15. Harrison,N.L., Majewska,M.D., Harrington,J.W. and Barker,J.L. (1987) Structure-activity relationships for steroid interaction with the gamma-aminobutyric acid A receptor complex. *J. Pharmacol. Exp. Ther.*, **241**, 346–353.
16. Rupprecht,R., Reul,J.M., Trapp,T., van,S.B., Wetzel,C., Damm,K., Zieglgansberger,W. and Holsboer,F. (1993) Progesterone receptor-mediated effects of neuroactive steroids. *Neuron*, **11**, 523–530.
17. Concas,A., Mostallino,M.C., Porcu,P., Follesa,P., Barbaccia,M.L., Trabucchi,M., Purdy,R.H., Grisenti,P. and Biggio,G. (1998) Role of brain allopregnanolone in the plasticity of gamma-aminobutyric acid type A receptor in rat brain during pregnancy and after delivery. *Proc. Natl Acad. Sci. USA*, **95**, 13284–13289.
18. Smith,S.S., Gong,Q.H., Hsu,F.C., Markowitz,R.S., French,M.J. and Li,X. (1998) GABA(A) receptor alpha4 subunit suppression prevents withdrawal properties of an endogenous steroid. *Nature*, **392**, 926–930.
19. Concas,A., Follesa,P., Barbaccia,M.L., Purdy,R.H. and Biggio,G. (1999) Physiological modulation of GABA(A) receptor plasticity by progesterone metabolites. *Eur. J. Pharmacol.*, **375**, 225–235.
20. Fujii,E. and Mellon,S.H. (2001) Regulation of uterine gamma-aminobutyric acid(A) receptor subunit expression throughout pregnancy. *Endocrinology*, **142**, 1770–1777.
21. Beato,M., Herrlich,P. and Schutz,G. (1995) Steroid hormone receptors: many actors in search of a plot. *Cell*, **83**, 851–857.
22. Mangelsdorf,D.J., Thummel,C., Beato,M., Herrlich,P., Schutz,G., Umesono,K., Blumberg,B., Kastner,P., Mark,M., Chambon,P. *et al.* (1995) The nuclear receptor superfamily: the second decade. *Cell*, **83**, 835–839.
23. Chambon,P. (1996) A decade of molecular biology of retinoic acid receptors. *FASEB J.*, **10**, 940–954.
24. Yamamoto,A., Hashimoto,Y., Kohri,K., Ogata,E., Kato,S., Ikeda,K. and Nakanishi,M. (2000) Cyclin E as a coactivator of the androgen receptor. *J. Cell Biol.*, **150**, 873–880.
25. Hovland,A.R., Powell,R.L., Takimoto,G.S., Tung,L. and Horwitz,K.B. (1998) An N-terminal inhibitory function, IF, suppresses transcription by the A-isoform but not the B-isoform of human progesterone receptors. *J. Biol. Chem.*, **273**, 5455–5460.
26. Glass,C.K. (1994) Differential recognition of target genes by nuclear receptor monomers, dimers and heterodimers. *Endocrinol. Rev.*, **15**, 391–407.
27. Yanagisawa,J., Yanagi,Y., Masuhiro,Y., Suzawa,M., Watanabe,M., Kashiwagi,K., Toriyabe,T., Kawabata,M., Miyazono,K. and Kato,S. (1999) Convergence of transforming growth factor-beta and vitamin D signaling pathways on SMAD transcriptional coactivators. *Science*, **283**, 1317–1321.
28. Watanabe,M., Yanagisawa,J., Kitagawa,H., Takeyama,K., Ogawa,S., Arao,Y., Suzawa,M., Kobayashi,Y., Yano,T., Yoshikawa,H., Masuhiro,Y. and Kato,S. (2001) A subfamily of RNA-binding DEAD-box proteins acts as an estrogen receptor alpha coactivator through the N-terminal activation domain (AF-1) with an RNA coactivator, SRA. *EMBO J.*, **20**, 1341–1352.
29. Khorasanizadeh,S. and Rastinejad,F. (2001) Nuclear-receptor interactions on DNA-response elements. *Trends Biochem. Sci.*, **26**, 384–390.
30. Tan,J.A., Marschke,K.B., Ho,K.C., Perry,S.T., Wilson,E.M. and French,F.S. (1992) Response elements of the androgen-regulated C3 gene. *J. Biol. Chem.*, **267**, 4456–4466.
31. Lydon,J.P., DeMayo,F.J., Funk,C.R., Mani,S.K., Hughes,A.R., Montgomery,C.J., Shyamala,G., Conneely,O.M. and O'Malley,B.W. (1995) Mice lacking progesterone receptor exhibit pleiotropic reproductive abnormalities. *Genes Dev.*, **9**, 2266–2278.
32. Schoenmakers,E., Verrijdt,G., Peeters,B., Verhoeven,G., Rombauts,W. and Claessens,F. (2000) Differences in DNA binding characteristics of the androgen and glucocorticoid receptors can determine hormone-specific responses. *J. Biol. Chem.*, **275**, 12290–12297.
33. Claessens,F., Verrijdt,G., Schoenmakers,E., Haelens,A., Peeters,B., Verhoeven,G. and Rombauts,W. (2001) Selective DNA binding by the androgen receptor as a mechanism for hormone-specific gene regulation. *J. Steroid Biochem. Mol. Biol.*, **76**, 23–30.
34. Wigley,W.C., Prihoda,J.S., Mowszowicz,I., Mendonca,B.B., New,M.I., Wilson,J.D. and Russell,D.W. (1994) Natural mutagenesis study of the human steroid 5 alpha-reductase 2 isozyme. *Biochemistry*, **33**, 1265–1270.
35. Takeyama,K., Kitanaka,S., Sato,T., Kobori,M., Yanagisawa,J. and Kato,S. (1997) 25-Hydroxyvitamin D3 1alpha-hydroxylase and vitamin D synthesis. *Science*, **277**, 1827–1830.
36. Mahendroo,M.S., Cala,K.M., Hess,D.L. and Russell,D.W. (2001) Unexpected virilization in male mice lacking steroid 5 alpha-reductase enzymes. *Endocrinology*, **142**, 4652–4662.
37. Mulac,J.B., Mullinax,R.A., DeMayo,F.J., Lydon,J.P. and Conneely,O.M. (2000) Subgroup of reproductive functions of progesterone mediated by progesterone receptor-B isoform. *Science*, **289**, 1751–1754.
38. Murayama,A., Takeyama,K., Kitanaka,S., Kodera,Y., Hosoya,T. and Kato,S. (1998) The promoter of the human 25-hydroxyvitamin D3 1 alpha-hydroxylase gene confers positive and negative responsiveness to PTH, calcitonin and 1 alpha,25(OH)2D3. *Biochem. Biophys. Res. Commun.*, **249**, 11–16.
39. Kodera,Y., Takeyama,K., Murayama,A., Suzawa,M., Masuhiro,Y. and Kato,S. (2001) Ligand type-specific interactions of peroxisome proliferator-activated receptor gamma with transcriptional coactivators. *J. Biol. Chem.*, **275**, 33201–33204.
40. Shen,R., Sumitomo,M., Dai,J., Hardy,D.O., Navarro,D., Usmani,B., Papandreou,C.N., Hersh,L.B., Shipp,M.A., Freedman,L.P. and Nanus,D.M. (2000) Identification and characterization of two androgen response regions in the human neutral endopeptidase gene. *Mol. Cell. Endocrinol.*, **170**, 131–142.
41. Matsui,D. (2001) GenBank accession no. AB049456.
42. Matsui,D. (2001) GenBank accession no. AB049455.
43. Rupprecht,R. and Holsboer,F. (1999) Neuroactive steroids: mechanisms of action and neuropsychopharmacological perspectives. *Trends Neurosci.*, **22**, 410–416.
44. Purdy,R.H., Morrow,A.L., Moore,P.J. and Paul,S.M. (1991) Stress-induced elevations of gamma-aminobutyric acid type A receptor-active steroids in the rat brain. *Proc. Natl Acad. Sci. USA*, **88**, 4553–4557.
45. Swain,A. and Lovell,B.R. (1999) Mammalian sex determination: a molecular drama. *Genes Dev.*, **13**, 755–767.

FERTILITY AND STERILITY®
*VOL. 73, NO. 6, JUNE 2000*

Published by Elsevier Science Inc.
Printed on acid-free paper in U.S.A.

# Characterization of messenger RNA expression of estrogen receptor-$\alpha$ and -$\beta$ in patients with ovarian endometriosis

*Sachiko Matsuzaki, M.D.,*[a] *Takao Fukaya, M.D.,*[a] *Shigeki Uehara, M.D.,*[a] *Takashi Murakami, M.D.,*[a] *Hironobu Sasano, M.D.,*[b] *and Akira Yajima, M.D.*[a]

*Tohoku University School of Medicine, Sendai, Japan*

**Objective:** To evaluate the expression of estrogen receptor (ER)-$\alpha$ and ER-$\beta$ messenger RNA (mRNA) in ovarian endometriosis.

**Design:** Prospective study.

**Setting:** University hospital.

**Patient(s):** Patients with endometriosis and patients with uterine leiomyoma or carcinoma in situ.

**Intervention(s):** A sample of ovarian endometriotic cyst tissue was obtained from each of the 32 patients during laparoscopic cystectomy. Samples of ovarian tissue and endometrium were obtained from 15 patients during or just after surgery.

**Main Outcome Measure(s):** Expression of mRNA for ER-$\alpha$ and ER-$\beta$ with use of the reverse transcription-polymerase chain reaction (RT-PCR) and nonradioactive in situ hybridization (ISH) techniques.

**Result(s):** Expression of mRNA for ER-$\alpha$ and ER-$\beta$ was observed in all of the control tissues from the normal endometrium and normal ovaries in the RT-PCR and ISH analyses, although the distribution of positive signals changed in the ISH analysis during different phases of the menstrual cycle. Messenger RNA for ER-$\alpha$ was detected in all of the ovarian endometriotic cysts analyzed (19 of 19), but mRNA for the ER-$\beta$ was limited (12 of 19) in the RT-PCR analysis. The ISH analysis confirmed the RT-PCR results and revealed that the two estrogen receptors were localized in both epithelial and stromal cells of endometriotic tissues.

**Conclusion(s):** The results suggest that predominant expression of ER-$\alpha$ in both glandular epithelial and stromal cells may be essential to the development and growth of ovarian endometriosis. (Fertil Steril® 2000; 73:1219–25. ©2000 by American Society for Reproductive Medicine.)

**Key Words:** Estrogen receptor-$\alpha$, estrogen receptor-$\beta$, in situ hybridization, ovarian endometriosis, reverse transcription-polymerase chain reaction

Received September 28, 1999; revised and accepted December 17, 1999.

Reprint requests: Sachiko Matsuzaki, M.D., Department of Obstetrics and Gynecology, Tohoku University School of Medicine, 1-1, Seiryo-machi, Aoba-ku, Sendai, 980-8574, Japan (FAX: +81-22-717-7258; E-mail: matsuzaki@ob-gy.med.tohoku.ac.jp).

[a] Department of Obstetrics and Gynecology.

[b] Department of Pathology.

0015-0282/00/$20.00
PII S0015-0282(00)00527-6

Endometriosis, one of the most common gynecological disorders, is defined as the presence of endometrial stroma and epithelium outside the uterine cavity (1). Lesions may appear in the ovary as endometriotic cysts, in which endometriotic foci are surrounded by a fibrous capsule that enlarges to form a cyst containing a dark-brown semifluid substance. Endometriosis occurs almost exclusively in menstruating women of reproductive age. It is highly likely, therefore, that estrogen stimulates the growth of endometriotic tissue.

It has been hypothesized that estrogen acts via a single receptor, the classical estrogen receptor (ER-$\alpha$) in the formation of endometriotic lesions. After the successful cloning of ER-$\alpha$ complementary DNA (cDNA) (2), many studies (3–8) were performed to examine the interaction between endometriotic lesions and ER-$\alpha$. Recently, a novel estrogen receptor, ER-$\beta$, was cloned (9, 10). The ER-$\beta$ messenger RNA (mRNA) expression has been detected in several organs, including testes and ovaries (11).

We analyzed the expression of ER-$\beta$ mRNA in normal endometrial tissues with use of the in situ hybridization (ISH) technique and charted the changes in expression throughout the menstrual cycle (12). To date, no studies have examined the localization of ER-$\beta$ mRNA expression in endometriotic lesions throughout the menstrual cycle. It is very important to determine the possible significance of the localization of both ER-$\alpha$ and

**TABLE 1**

Sequences of primers and hybridization probes for ER-α and ER-β mRNA.

| | | |
|---|---|---|
| ER-α | TGTGCAATGACTATGCTTCA | 852–871 |
| | GCTCTTCCTCCTGTTTTTA | 982–1,000 |
| | CAGCTCGTTCCCTTGGATCTGATGCAGTAG[a] | 332–361 |
| ER-β | GTCCATCGCCAGTTATCACATC | 130–151 |
| | GCCTTACATCCTTCACACGA | 352–371 |
| | TGTTGGCCACAACACATTTGGGCTTGTGGT[a] | 76–105 |

[a] Sequences of hybridization probes.

*Matsuzaki. ER-α and -β in endometriosis. Fertil Steril 2000.*

ER-β mRNA expression in the development and growth of endometriotic lesions.

In the present study, we used the reverse transcription-polymerase chain reaction (RT-PCR) method to evaluate the expression of both ER-α and ER-β mRNA in ovarian endometriotic cysts. On the basis of the results of the RT-PCR analyses, we used the nonradioactive ISH technique to attempt to identify the localization of mRNA for ER-α and ER-β.

## MATERIALS AND METHODS

### Experimental Subjects

During laparoscopic cystectomy, a sample of ovarian endometriotic cyst tissue was obtained from each of the 32 patients (20–39 years of age) participating in this study. They received no hormonal treatment, such as GnRH agonist (GnRH-a) or sex steroids, during the minimum 6 months period preceding surgery and had regular menstrual cycles, which were determined by their menstrual history and measurement of serum 17β-estradiol and progesterone levels. Fifteen patients were in the follicular phase, and 17 were in the luteal phase. With use of the revised American Fertility Society classification scheme (13), we determined the endometriotic stage for each sample. Twenty-three of the samples were identified as class III, whereas the remaining 9 samples were identified as class IV. All of the endometriotic cysts were more than 3 cm in diameter and contained a grandular epithelium surrounded by stromal tissue. The presence of these features was sufficient to meet the criteria for histopathologic diagnosis of endometriosis.

Control tissue samples were obtained from a total of 15 subjects. First, we obtained samples (n = 9) of normal eutopic endometrium: 3 in the proliferative phase, 2 in the early secretory phase, 2 in the midsecretory phase, and 2 in the late secretory phase, as determined by the criteria of Noyes et al. (14). We then obtained biopsy samples (n = 6) of normal ovarian tissue: 3 in the follicular phase and 3 in the luteal phase. The control samples were collected from patients without endometriosis who had never received hormonal therapy but had undergone hysterectomy due to uterine leiomyoma or carcinoma in situ of the uterine cervix.

Each of the fresh tissue samples was divided into two portions. The first tissue portion was fixed in 4% paraformaldehyde (pH 7.4) and embedded in paraffin to permit the ISH analysis of mRNA from ER-α and ER-β. The second portion was immediately frozen in liquid nitrogen and stored at −80°C until it was used in the RT-PCR analysis. All of the tissue samples were obtained with the patient's full informed consent. The human research board of the ethics committee of Tohoku University School of Medicine approved the research protocol.

### Oligodeoxynucleotide Primers and Probes for ER-α and ER-β

Oligodeoxynucleotide primers for the RT-PCR analysis of ER-α and ER-β mRNA were designed with use of the published sequences (15). The PCR product derived from ER-α mRNA was expected to be 149 bp, whereas that of ER-β mRNA was expected to be 242 bp.

Oligodeoxynucleotide probes with a 3′-biotinylated tail (Brigati tail; 5′-probe-biotin-biotin-biotin-TAG-TAG-biotin-biotin-biotin-3′) were designed for the ISH of ER-α and ER-β mRNA. The methods involved in this procedure were previously described (12, 16). This avoids cross-hybridization, which might otherwise occur because of the similarity between nucleotide sequences of the two ER genes, with other steroid receptor genes. Table 1 lists the primer and probe sequences and the locations of the cDNA corresponding to the human ER-α (2) and ER-β (10). Figure 1 shows the schematic representation of the structures of the ER-α and ER-β coding regions (complementary DNA) and the locations of the primers.

### Extraction of RNA and RT-PCR Analysis

Of the 32 endometriotic tissue samples originally intended for the RT-PCR analysis, 19 were included in the

**FIGURE 1**

Schematic representation of the structures of the ER-α– and ER-β–coding regions (complementary DNA) and the locations of the primers used for RT-PCR analysis. The positions of the translation initiation (ATG) and termination (TGA) codons are indicated. Black rectangles indicate the primer locations. Exon boundaries are shown as vertical bars. F = forward primer; R = reverse primer.

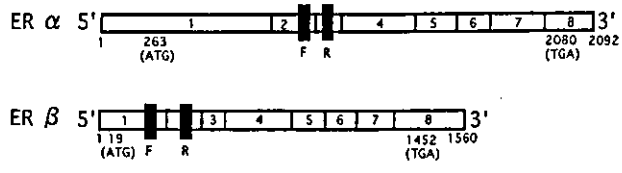


*Matsuzaki. ER-α and -β in endometriosis. Fertil Steril 2000.*

final analysis. Of the 19 samples, 9 were in follicular phase and 10 were in luteal phase. The remaining 13 samples were excluded from the RT-PCR analysis because they appeared to be contaminated with normal ovarian tissue.

Each of the frozen tissue samples subjected to the RT-PCR analysis was first homogenized, and the total RNA was extracted with ISOGEN (Nippon Gene, Toyama, Japan), according to the manufacturer's instructions. The cDNA was reverse transcribed at 42°C for 50 minutes in 19 μL of reaction solution containing 1 μg of total RNA, 2.5 mM $MgCl_2$, 5 mM 1,4-dithiothreitol (Cleland's reagent) (DTT), 0.5 mM dNTPs (0.5 mM each dATP, dCTP, dGTP, and dTTP), random hexamers (50 ng/mL) (GIBCO BRL, Tokyo, Japan), and 200 U of Superscript II RT (reverse transcriptase; GIBCO BRL). As a negative control, 1 μL of dietylpyrocarbonate-treated distilled water, with no RNA contamination, was subjected to the same RT reaction.

The PCR was performed thereafter in a 50-μL volume of the final reaction solution containing 2 μL of the RT reaction product, 5 μL of 10× PCR buffer, 2.5 mM $MgCl_2$, 0.5 mM dNTPs, 0.4 μM of each of the sense and antisense primers for ER-α or ER-β, and 2.5 U Taq DNA polymerase (Takara, Otsu, Japan). Amplification was performed in a PCR thermocycler (Takara) with use of a hot start. The same cycle profiles were used for both ER-α and ER-β. The cycles began with an initial denaturation period at 94°C for 5 minutes, followed by 35 cycles at 94°C for 1 minute, 60°C for 1 minute, and 72°C for 1.5 minutes, with a final extension period at 72°C for 10 minutes. As an external positive control to test the integrity of the RT-PCR process, expression of β-actin mRNA was evaluated in each RT reaction product under the following amplification profile: 95°C for 1 minute, followed by 35 cycles of 94°C for 1 minute, 58°C for 1 minute, and 72°C for 2 minutes. The PCR products were subjected to electrophoresis on 2% agarose gels and visualized by ethidium bromide staining. All RT-PCR procedures were performed at least twice in separate experiments.

## In Situ Hybridization of ER-α and ER-β

Serial thin sections (3 μm) of paraffin-embedded tissues were cut and mounted on Probe-On glass slides (Fisher Scientific, Pittsburgh, PA). The ISH was performed with a manual capillary action system (MicroProbe staining system, Fisher Scientific) using a modified version of the methods reported previously (12, 16–18). Tissue sections were rapidly dewaxed, cleared with Auto-alcohol (Research Genetics, Huntsville, AL), rehydrated with a Tris-based buffer, pH 7.4 (Research Genetics), and digested with pepsin (2.5 mg/mL, Research Genetics) for 4 minutes at 105°C. The probe in formamide-free diluent was applied to the sections. The slides were heated to 105°C for 3 minutes, cooled for 1 minute at room temperature, and allowed to hybridize at 45°C for 45 minutes. Thereafter, the sections were washed three times with 2× SSC (standard saline citrate) at room

**FIGURE 2**

The RT-PCR detection of ER-α and ER-β mRNA in two samples of ovarian endometriotic tissues. The molecular sizes of the specific bands are indicated. Bands, of which molecular sizes were <100 bp, were derived probably from primer dimers. (**A**), from case no. 6 and (**B**) from case no. 19 in Table 3. M = molecular size marker (100-bp ladder); *lane 1*, RT-PCR for ER-α mRNA; *lane 2*, for ER-β mRNA; *lane 3*, for β-actin mRNA; and *lane 4*, negative control without RT.

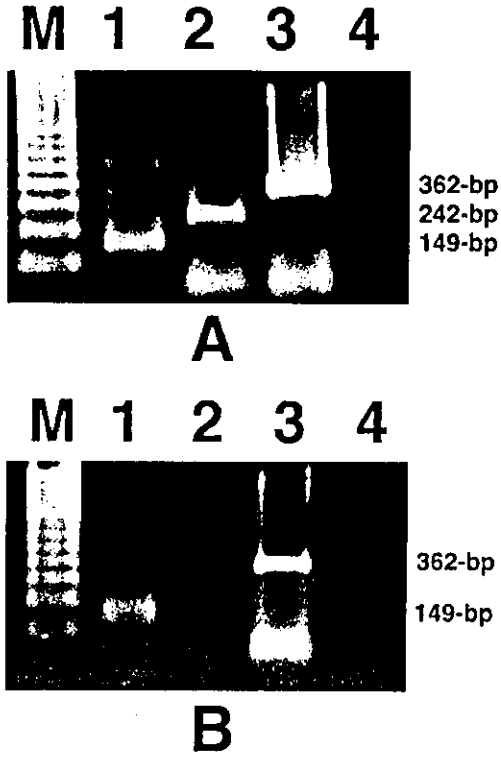


*Matsuzaki. ER-α and -β in endometriosis. Fertil Steril 2000.*

temperature and incubated with alkaline phosphate-conjugated streptavidin (Research Genetics). After the sections were washed, they were treated in AP chromogen buffer (pH 9.5, Research Genetics) at room temperature, and hybridization signals were visualized with use of fast red salt (Research Genetics). The sections were counterstained with hematoxylin, air dried, and coverslipped for microscopic observation.

Fetal kidney tissues, in which moderate expression of ER-β mRNA has been proven by RT-PCR (19), were used as positive controls. Negative control experiments were performed with use of sense probes that had complementary sequences to one of the antisense probes. The results are shown as the relative intensity of mRNA hybridization signals. They have been classified as either "no signal over background," "equivocally positive signal," or "positive signal."

**TABLE 2**

Results of RT-PCR and in situ hybridization study for ER-α and ER-β in normal ovaries.

| | ER-α | | ER-β | |
|---|---|---|---|---|
| | RT-PCR | ISH | RT-PCR | ISH |
| Stage | | SE | | SE |
| Follicular (n = 3) | + | + | + | + |
| Luteal (n = 3) | + | + | + | + |

*Note:* Signal intensity was classified into three categories. − = no signal over background; +/− = equivocally positive signal; + = positive signal. SE = surface epithelium.

*Matsuzaki. ER-α and -β in endometriosis. Fertil Steril 2000.*

## RESULTS

### Reverse Transcription-Polymerase Chain Reaction Analysis of ER-α and ER-β

The results are shown in Figure 2 and in Tables 2–4. We detected the expected 149-bp product for ER-α mRNA and the 242-bp product for ER-β mRNA in the normal eutopic endometrium and in the tissues sampled from normal ovaries. The products could be detected regardless of the phase of the menstrual cycle during which the samples were obtained. Messenger RNA for ER-α was detected in all (19 of 19) of the endometriotic cyst tissue samples, but expression of mRNA for ER-β was limited to 12 of 19 (63%) of the samples. No difference was observed in ratios of positive-negative expression of ER-β mRNA between samples identified to be in the follicular phase vs. the luteal phase (6 cases of positive expression and 3 cases of negative expression in the follicular-phase samples compared with 6 cases of positive expression and 4 cases of negative expression in the luteal-phase samples).

**TABLE 3**

Results of RT-PCR and in situ hybridization study for ER-α and ER-β in the functionalis of eutopic endometrium.

| | ER-α | | | ER-β | | |
|---|---|---|---|---|---|---|
| | | ISH | | | ISH | |
| Endometrial dating | RT-PCR | G | S | RT-PCR | G | S |
| Proliferative (n = 3) | + | + | + | + | + | + |
| Early secretory (n = 2) | + | + | +/± | + | + | ±/− |
| Midsecretory (n = 2) | + | +/± | +/± | + | ±/− | ±/− |
| Late secretory (n = 2) | + | ±/− | ±/− | + | ±/− | ±/− |

*Note:* Signal intensity was classified into three categories. − = no signal over background; ± = equivocally positive signal; + = positive signal. G = glandular epithelium; S = stroma.

*Matsuzaki. ER-α and -β in endometriosis. Fertil Steril 2000.*

**TABLE 4**

Results of RT-PCR and in situ hybridization study for ER-α and ER-β mRNA in ovarian endometriosis.

| | | ER-α | | | ER-β | | |
|---|---|---|---|---|---|---|---|
| | | | ISH | | | ISH | |
| Case no. | Stage | RT-PCR | G | S | RT-PCR | G | S |
| 1 | F | + | + | + | + | + | + |
| 2 | F | + | + | + | − | − | − |
| 3 | F | + | + | + | − | − | − |
| 4 | F | + | + | + | + | − | − |
| 5 | F | + | ± | ± | + | − | − |
| 6 | F | + | + | + | + | + | + |
| 7 | F | + | + | + | − | − | − |
| 8 | F | + | ± | ± | + | + | ± |
| 9 | F | + | + | + | + | ± | + |
| 10 | F | ND | + | + | ND | + | ± |
| 11 | F | ND | + | ± | ND | + | + |
| 12 | F | ND | + | + | ND | − | − |
| 13 | F | ND | ± | + | ND | − | − |
| 14 | F | ND | + | + | ND | − | − |
| 15 | F | ND | + | + | ND | + | + |
| 16 | L | + | ± | ± | − | − | − |
| 17 | L | + | + | + | + | ± | + |
| 18 | L | + | + | + | + | + | ± |
| 19 | L | + | + | + | − | − | − |
| 20 | L | + | + | + | − | − | − |
| 21 | L | + | + | + | − | − | − |
| 22 | L | + | + | ± | + | + | ± |
| 23 | L | + | + | + | + | ± | + |
| 24 | L | + | ± | + | + | − | − |
| 25 | L | + | + | + | + | + | ± |
| 26 | L | ND | + | + | ND | − | − |
| 27 | L | ND | ± | ± | ND | + | + |
| 28 | L | ND | + | + | ND | − | − |
| 29 | L | ND | ± | + | ND | + | ± |
| 30 | L | ND | + | + | ND | − | − |
| 31 | L | ND | + | + | ND | − | − |
| 32 | L | ND | + | + | ND | ± | + |

*Note:* Signal intensity was classified into three categories. − = no signal over background; ± = equivocally positive signal; + = positive signal. F = follicular phase in menstrual cycle; L = luteal phase in menstrual cycle; ND = analyses were not performed, because there was evidence that samples were contaminated by normal ovarian tissue; G = glandular epithelium; S = stroma.

*Matsuzaki. ER-α and -β in endometriosis. Fertil Steril 2000.*

### In Situ Hybridization of ER-α and ER-β

The results of the ISH analysis are shown in Figures 3 and 4 and in Tables 2–4. In the proliferative phase eutopic endometrium, ER-α mRNA was expressed in both glandular epithelial and stromal cells, whereas ER-β mRNA was expressed predominantly in glandular epithelial cells. Although the same pattern was observed in the secretory phase, both ER-α and ER-β mRNA expression in glandular epithelial and stromal cells were markedly decreased with the progression of the secretory phase.

In contrast, ovarian surface epithelial cells uniformly ex-